



Investor Expectations and the Covid-19 Stock Market Crash. What Can We Learn From Index Options?

**A Replicating Study of David Bates' The Crash of '87: Was it
Expected? The Evidence from Options Markets.**

Caroline Marie Andersen & Maren Risvik

Supervisor: Jørgen Haug

Master's Thesis, Master of Science in Economics and Business
Administration, Financial Economics

NORWEGIAN SCHOOL OF ECONOMICS

This thesis was written as a part of the Master of Science in Economics and Business Administration at NHH. Please note that neither the institution nor the examiners are responsible – through the approval of this thesis – for the theories and methods used, or results and conclusions drawn in this work

Abstract

We investigate the transaction prices of SPX options on the S&P 500 Composite Index over the years 2018 to 2020, to examine whether there can be shown evidence of expectations of a market crash before February 20, 2020. This is done by replicating the methods used in David Bates' "The Crash of '87: Was it Expected? The Evidence from Options Markets". First, we show that out-of-the-money put options were trading at a premium relative to out-of-the-money call options during most of the period examined. In the beginning of the crisis this premium decreased, and it was not until March 16, 2020, that the market participants began to buy protection. Second, we estimate jump-parameters implicit in SPX option prices based on Bates' model of option pricing under an asymmetric jump-diffusion. The results indicate that there was no unnormal expectancy of jumps before the crash occurred in February. We find no evidence of a reaction in market expectations until mid-March. The same is true for the calculated implied volatility, skewness and kurtosis of the underlying return distribution. Hence, we conclude that both methods find no evidence of increased crash fears prior to the market crash beginning on February 20, 2020. We find that the full impact of the crisis is not observed in market expectations elicited from SPX option prices until March 2020.

Acknowledgements

This master thesis is part of our MSc in Economics and Business Administration, with a major in Financial Economics. The writing process has been challenging, interesting and highly educational.

First of all, we would like to extend our sincere gratitude to our supervisor Jørgen Haug for excellent guidance, ideas and insights during the semester. Despite the difficulties due to the Covid-19 outbreak, he has been available whenever we needed assistance.

Second, we would like to thank NHH for providing access to databases and software that have been highly useful for our study.


We also want to thank our friends and fellow students for making our time at NHH memorable.

Finally, we would like to extend our warmest gratitude to our families for the endless support.

Date: 19. December 2020, Norway

Caroline Marie Andersen

Maren Risvik





Contents

Abstract	i
Acknowledgements	ii
List of Figures	iv
List of Tables.....	v
1. Introduction	1
2. Data	6
3. Part 1: Measures of Asymmetry Under Standard Distributional Hypothesis	9
3.1 Theory.....	9
3.2 Methodology.....	16
3.3 Analysis	20
4. Part 2: Option Pricing Under Asymmetric Jump-Diffusion Processes	23
4.1 Theory.....	23
4.2 Methodology.....	30
4.2.1 Sample Restrictions	30
4.2.2 Estimation Model	30
4.2.3 Implied Volatility, Skewness and Kurtosis	35
4.3 Analysis	36
4.3.1 The Estimated Jump Parameters	36
4.3.2 Implied Volatility, Skewness and Kurtosis	40
5. Limitations.....	44
6. Conclusions	47
References	48

List of Figures

Figure 1. The S&P 500 index.....	3
Figure 2. Total open interest of SPX put and call options.	8
Figure 3. Risk-neutral distribution with no skewness.....	11
Figure 4. Risk-neutral distributions with positive and negative skewness.	12
Figure 5. Estimated splines for puts and calls.....	17
Figure 6. The daily mean standard errors of the cubic spline interpolation of calls and puts.....	19
Figure 7. The daily skewness premia of ATM and 4% OTM options.	20
Figure 8. Zoomed plot of 4 % OTM options skewness premia, January–May 2020.....	21
Figure 9. Random combinations of start-parameters.	34
Figure 10. Risk-neutral expected number of jumps per year and the price of the S&P500...	37
Figure 11. Implicit jump standard deviation of jump size and the S&P 500 index	38
Figure 12. The risk-neutral mean jump size (conditional on a jump) and the SPX.	38
Figure 13. The risk-neutral expected value of jumps per year and the S&P 500 index.....	39
Figure 14. The risk-neutral expected value of jumps per year, zoomed	39
Figure 15. The implicit skewness of the risk-neutral distribution of the S&P 500 index.....	42
Figure 16. Risk-neutral expected value of jumps per year and the implicit skewness.	42
Figure 17. The implicit kurtosis of the risk-neutral return distribution of the S&P 500 index, and the index level.....	43
Figure 18. The estimated implied volatility and the VIX index.....	43

List of Tables

Table 1. Summary statistics of the data.....	7
Table 2. Summary of the option data.	8
Table 3. Skewness premium under different classes of distributional hypotheses.	15
Table 4. Theoretical option prices.	33

1. Introduction

In 1987, the U.S. stock market experienced a crash, which subsequently resembled a bubble as it followed after a large gain in the market. Bates (1991) explores the hypothesis that the market crash in 1987 happened because the market expected it to happen, a so-called rational bubble. He examines the market expectations from 1985 to 1987 and two approaches are used in the study.

First, the skewness premium is defined as the relative prices of the call option, c , and the corresponding put option, p ; $\frac{c-p}{p}$. The skewness premium of 4% out-of-the-money (OTM) options on futures on the S&P 500 index (SPX) is studied over time, to investigate whether the market expected a crash before it occurred. If the skewness premium is negative, it may imply that market participants either expect a crash, or that they expect the return volatility to increase if the market falls. The theoretical framework of this approach is discussed further in Section 3.1.

Second, he creates a model for pricing options under a jump-diffusion. His model for the price of the underlying asset is different from earlier work that was done in this field, in that he allows the random jumps to be asymmetric. Hence, allowing them to have mean different from zero. It also differs from the previous work in that the price of the jump risk is not assumed to be 0, meaning that he allows the jump risk to be systematic. From this model he finds the daily jump parameters implicit in the option transaction prices through nonlinear least squares. As discussed further in Section 4.1, these parameters can be used to draw inferences about the market expectations of jumps. The parameters are:

- the jump intensity parameter
- the mean jump size, conditional on the occurrence of a jump
- the standard deviation of jump size, conditional on the occurrence of a jump
- the volatility, conditional on no jump occurring

He observes that the mean jump size becomes predominantly negative after October 1986. The expected value of jumps per year, defined as the jump intensity times the mean jump size, becomes largely negative. The monthly skewness calculated using the estimated jump-diffusion parameters also becomes negative at this point, after being positive from January 1985 until October 1986.

Hence, the changes in the jump-parameters implicit in the option prices imply that crash fears begin to increase a year preceding the crash. He also finds that when the market peaks in August 1987, the crash fears fall as the implicit parameters and skewness move back to normal levels. Bates' model for pricing options under a jump-diffusion and the theoretical foundations of this second approach is discussed further in Section 4.1.

The study concludes that the market did in fact expect either negative jumps or that the volatility of return would increase should there be a fall in the market. The evidence of these expectations began a year preceding the crash, but they ended 2 months before the market actually fell. From this he concludes that "if there was a rational bubble in the stock market, one would have to conclude that it burst in mid-August – not in mid-October" (Bates, 1991, p. 1037).

In our study, we use the methods of Bates (1991) to extract the market participants' expectations of jumps from SPX option prices, before and during the Covid-19 stock market crash. The objective of our thesis is therefore to examine the following question:

Do the SPX option prices show evidence of changes in the market expectations of negative jumps before the actual Covid-19 stock market crash?

From the World Health Organization (WHO) Covid-19 official timeline, it follows that on December 31, 2019, Wuhan Municipal Health Commission reported a cluster of cases of a pneumonia in Wuhan. A new coronavirus was identified eventually. The first recorded case outside of China was confirmed in Thailand on January 13, 2020, and the first confirmed case in the U.S. was on January 20. In February 2020 there was a flow of new cases, and in March 2020 the worsening continued. On March 11, WHO made an assessment that Covid-19 could be characterized as a pandemic. The S&P 500 had its largest daily drop on March 11. In March, the U. S. passed a stimulus package of about \$2.2 trillion. On April 4, WHO reported that there were over 1 million confirmed cases of COVID-19 worldwide, and that there had been more than a tenfold increase in less than a month. The S&P 500 index started falling after February 19, 2020 and reached its lowest point of \$2,237.4 on March 23 after a fall of 34 %. The index price during 2018 – 2020 is illustrated in Figure 1, highlighting the dates mentioned above.



Figure 1. The S&P 500 index. The S&P 500 index price over the period January 2018 – October 2020. The index started falling after 19th of January 2020, and reached its lowest point of \$2,237.4 on March 23, after a fall of 34 %. The index price did not seem to react on the first case of Covid-19 outside of China, reported the 13th of January. We observe a relatively small decrease after the 20th of January, when the first case in the U.S. was confirmed. The 11th of March, World Health Organization made the assessment that Covid-19 should be characterized a pandemic. The 16th of March, the S&P 500 had its largest daily drop.

The market crash of 1987 is presumed to be precipitated by trading models driven by computers that followed a portfolio insurance strategy. Precursors are thought to be several monetary and foreign trade agreements depreciating the U.S. dollar to adjust the trade deficit, for then trying to make the dollar stable at the new lower level (Segal, 2020). However, as there were no major news events released the preceding weekend, the drop in the stock market on Black Monday cannot be attributed to any single news event. It was several events that ended up creating panic among the investors, which again lead to a major drop in the stock market. The Covid-19 crisis was in contrast not caused by financial factors, but by a new disease hindering companies to do business as usual, thus able to create a worldwide recession. As the S&P 500 index did not begin to fall until February 20, it is interesting to investigate whether market participants expected the fall beforehand.

Whereas Bates used American options on futures on the S&P 500, we use European options on the index to get a picture of the investor expectations of jumps. Bates used American options due to the fact that the major exchange-traded options on market indexes at that time were American. Today, index options are typically European. By using European options, we avoid the problem that stems from the early exercise premium in American option prices. We can then use options directly on the index, and the option pricing becomes less complicated. This is further discussed in Section 3.1.

First, we investigate the skewness premium of at-the-money (ATM) and 4 % OTM options from 2018-2020. From the OTM skewness premium, we can make inferences about whether market participants seemed to anticipate a market crash before it occurred. We observe that the put options typically trade at a premium above the call options, yielding a negative skewness premium. We find no evidence of reactions in the expectations prior to February 20. At this point, the skewness premium becomes *less* negative, meaning that the OTM put options become less expensive relative to the corresponding OTM call options. This trend continues until March 16, the day when the S&P 500 has its largest daily drop, when the skewness premium begins to decrease. Hence, it is at this point that the market participants buy insurance to protect themselves from a falling market. It implies that the market participants expect negative jumps, or that the volatility of returns will increase if the market fall (Bates, 1991, Proposition 1). We thus find that the full impact of the crisis is not observed in investor expectations until mid-March. As will be discussed below, this is consistent with other studies using forward-looking data to extract market expectations during the Covid-19 crisis.

Second, we use Bates' (1991) option pricing model under an asymmetric jump-diffusion process to estimate the daily implicit jump intensity, the mean jump size and jump dispersion through optimization. From this, we calculate the implied volatility and coefficients of skewness and kurtosis of the risk-neutral return distribution of the S&P 500 index. We then observe the changes over time, to see whether there is evidence of increasing crash fear before the stock market fall. We also compare the estimates to the Volatility Index (VIX) to observe whether they capture the same information about expectations of negative jumps.

We find that it is not until mid-March that the mean jump size decreases significantly and the expected number of jumps per year increases, making the expected value of jumps per year excessively negative. Hence, by observing the changes in the estimated parameters during the

time period January 2018 - October 2020, we find that there is no sign of increasing crash fears prior to February 20, 2020. In fact, we do not observe evidence of significant changes in market expectations of jumps until March 2020. This is consistent with the results found in Part 1 of the study. The calculated skewness of the underlying, risk-neutral return distribution increases in the beginning of the market crash, as the observed skewness premium in Part 1. It does on the other hand not decrease until April 2020.

The thesis is structured into two parts. The first method from Bates (1991) is elaborated and analyzed in Part 1, followed by Part 2 which addresses the second method. Both parts contain their own theory, methodology and analysis, before coming together to a conclusion at the end. We find that both methods show no evidence of a reaction in market participants' expectations of negative jumps prior to the Covid-19 stock market crash.

2. Data

We use the transaction prices of SPX options with the underlying being \$100 times the S&P 500 Composite Index, downloaded from Thomson Reuters Datastream. We also download the open interest and volume traded. The datasets are uploaded to R, which is the program we use to do our analysis. We examine daily data from January 2018 to October 2020, and only the prices that change from the preceding day are included as these are the prices of actual transactions. The options are European with cash settlement and the strike prices vary between 5-point and 10-point intervals.

For SPX options, the expiration months are up to twelve near-term months and the Exchange may in addition list up to ten expiration months between twelve to sixty months. The expiration days are the third Friday of the expiration month and all available maturities are downloaded. We impose similar restrictions for the data as Bates (1991). This is done to remove days of thin trading, options with short maturities as they do not contain enough information about the distribution and for efficiency gains. Thus, when examining the data, each day we only use the options that have time to maturity between 28 – 118 days. We remove the deepest out-of-the-money and in-the-money options. In addition, we only include data from days with at least 20 transactions in calls and 20 in puts. For these transactions, we require 4 different strike prices for calls and 4 for puts. We ensure strike price variation to distinguish amongst alternative distributional hypotheses. The intuition for why sufficient strike price variation is needed stems from the theory presented in Section 3.1. We need options in-, at- and out-of-the-money to get an understanding of the characteristics of the underlying distribution. Of the days included in the downloaded dataset, which had some missing days, there were 26 days that did not meet the transaction requirement. The remaining days had an efficient number of transactions as well as variety in strike prices.

Before imposing the above restrictions, the downloaded dataset contains prices of about 45 % calls and 55 % puts. From January 1, 2018, to October 1, 2020, there are 719 days of data. In contrast, for the available open interest, there is data of about 50 % calls and 50 % puts. Hence, there is missing data for both days and option prices. Note that if there are no options missing from the available open interest data, there is about the same number of calls and puts available in the market. We use this data to investigate the total open interest each day for puts and calls. From Figure 2 we observe that the open interest for puts is higher than for calls, during the

entire observed time period (assuming this holds for the missing days as well). This suggests that the demand is higher for put options than for call options. As we will discuss later, this might be the reason why we observe that put options are more expensive than corresponding call options during the observed time period.

After the above restrictions are imposed, we are left with 12,752 options observed over 684 days. On the day with the maximum options traded there are transactions in 1219 options, while the minimum had transactions in 355 options. On average, there are transactions in about 846 options per day. The strike prices vary between 1740 to 3860. About 45 % of the remaining options are calls, while about 55 % are puts. A summary of the remaining data is presented in Table 1 and Table 2. We make further restrictions on the data for Part 2 of the study, which is discussed in Section 4.2.1.

We use the daily middle rate of the bid and ask on 10-year US Treasury Bond as the riskless interest rate. This, together with the daily price and dividend-yield of the S&P 500 index, is downloaded from Thomson Reuters Datastream as well. At last, we download the closing value of the VIX index from Yahoo! Finance.

Data	Mean	Maximum	Minimum
VIX Index	19.902	82.690	9.150
S&P 500 Index	2904.831	3580.840	2237.400
Dividend yield	0.019	0.028	0.016
Riskless rate	0.021	0.032	0.005
Daily options traded	846.354	1219.000	355.000
Strike price	2720.550	3860.000	1740.000

Table 1. Summary statistics of the data. Summary of the mean, maximum and minimum values of the price of the VIX index, the S&P 500 index and its dividend yield, as well as the riskless rate, the number of options traded and corresponding strike prices during 2018-2020. The daily options traded, and strike prices are found from the options remaining after the discussed data restrictions are imposed.

Options	Calls	Puts
12752	45.10%	54.90%

Table 2. Summary of the option data. After the restrictions are imposed, we are left with 12,752 options. About 45 % of these are call options, while the remaining 55 % are put options.

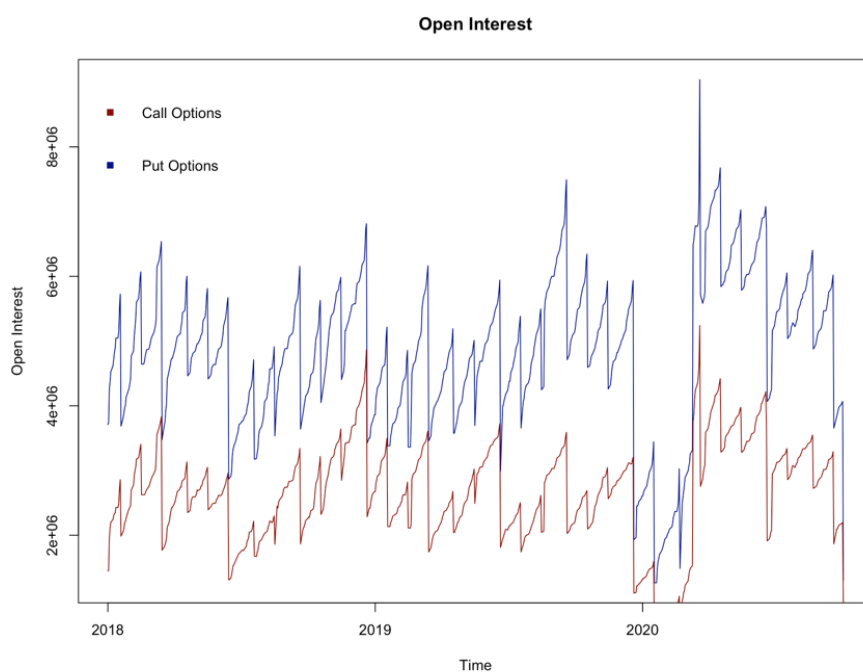


Figure 2. Total open interest of SPX put and call options. It shows the open interest for each day before the data restrictions are imposed, during 2018-2020. There is about the same number of calls and puts in the open interest data.

3. Part 1: Measures of Asymmetry Under Standard Distributional Hypothesis

In Section 3 we examine the skewness premium of options on the S&P 500 index. We wish to investigate whether it shows evidence of reactions in market expectations of negative jumps before the index falls. Section 3.1 contains the definition of the skewness premium as well as the theory explaining how we can use it to extract the relevant investor expectations. The methodology is presented in Section 3.2, followed by an analysis and conclusion of the findings in Section 3.3.

3.1 Theory

We use the skewness premium of OTM call and put options on the S&P 500 index to measure the changes in market participants' expectations of jumps. The definition of the skewness premium using European options is as follows: "The x % skewness premium is defined as the percentage deviation of x % out-of-the-money call prices from x % out-of-the-money put prices" (Bates, 1991, p. 1015):

$$SK(x) \equiv \frac{c(S,T;X_c)}{p(S,T;X_p)} - 1 \quad \text{for European options in general,} \quad (1)$$

, where:

$$X_p = \frac{F}{1+x} < F < X_c = F(1+x), \quad x > 0,$$

F is the forward price of the underlying asset, X is the option strike price, while T is the maturity.

When using the differences in call and corresponding put prices as a measure of market participants' expectations, we are in fact trying to measure the skewness in the risk-neutral distribution of the underlying asset. This is based on the fact that the price of an option equals its expected future payoff discounted using its expected rate of return. Given no arbitrage opportunities, we obtain the same price when using the expected payoff with risk-neutral probabilities and discounting using the riskless rate of return (r): $P = \frac{E(CF)}{\mu} = \frac{E^*(CF)}{r}$.

As the expected return is unknown and difficult to estimate, deriving the risk-neutral distribution is fundamental to the pricing of options. The risk-neutral distribution is often derived by replication using a dynamic trading strategy in a riskless bond and the underlying. This holds for processes such as the geometric Brownian motion with constant elasticity of variance when assuming no arbitrage, as the options are now redundant assets. This is not possible for more complex processes where pricing of volatility risk or jump risk is required. Then, the risk-neutral distribution is often found by assuming that the jump risk has a price of 0, thus assuming it is idiosyncratic, or restrictions on the utility function of the representative investor. In our case, having a wide market index as the underlying asset, it is not reasonable to argue that the jump risk is idiosyncratic. How we price options under a jump-diffusion allowing for systematic jump risk is presented in Section 4.1.

When having obtained the risk-neutral probabilities from this risk-neutral distribution, the European call and put options are priced by the following equations (Bates, 1991, p. 1012-1013):

$$\begin{aligned} c(S_t, T; X_c) &= e^{-r(T-t)} E_t^*(\max(S_T - X_c, 0)) \\ &= e^{-r(T-t)} E_t^*(S_T - X_c | S_T \geq X_c) Prob^*(S_T \geq X_c) \end{aligned} \quad (2)$$

$$\begin{aligned} p(S_t, T; X_p) &= e^{-r(T-t)} E_t^*(\max(X_p - S_T, 0)) \\ &= e^{-r(T-t)} E_t^*(X_p - S_T | S_T \leq X_p) Prob^*(S_T \leq X_p) \end{aligned} \quad (3)$$

,where:

T-t = the time left to maturity measured in years

r = the riskless rate assumed to be constant over the life of the option

S_T = the price of the underlying asset at maturity

If the European options end up ATM, their strike price equals the price of the underlying at the expiration date. Hence, there is no gain or loss when selling (buying) the underlying instead of choosing to exercise the put (call) option. If the put (call) ends up in-the-money (ITM), the strike price is higher (lower) than the underlying price at maturity, thus there is a gain associated with choosing to exercise the option. The opposite is true if the option ends up

OTM. The price of the option thus depends on the probability of whether the option will end up ITM, which we observe in the price equations above. This probability depends on the future value of the underlying asset. The future value is determined by the forward price. Under risk-neutrality and assuming that the riskless rate is independent of the underlying price, we have that: $F_{t,T} = E_t^*(S_T)$, i.e., the forward price equals the expected future value of the underlying. By arbitrage we have that $F_{t,T} = S_t e^{b(T-t)}$, where S_t is the value of the underlying asset at time t and b is the cost of carry. In our case the underlying asset is the S&P 500 index, hence the cost of carry is the riskless interest rate less the dividend yield. It measures the alternative cost of holding the stock instead of the riskless asset.

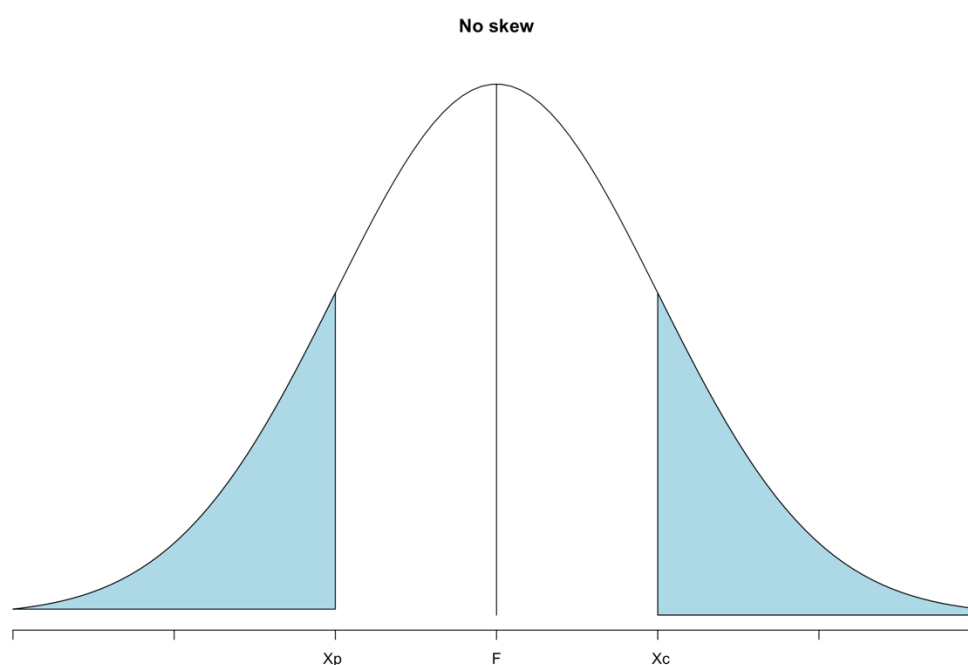


Figure 3. Risk-neutral distribution with no skewness. The strike prices are symmetrically around the forward price. As we observe, with no skew the OTM options should be priced the same, as the risk-neutral probabilities of the options ending up in-the-money, the blue areas, are exactly the same.

If the strike price of the call (put) option is lower (higher) than the current forward price with corresponding T , the option is more likely to end up ITM and will consequently be worth more than the option likely to end up OTM. Naturally, the deeper ITM the option gets, the higher the option price, and opposite.

From this it follows that OTM European call options are linked to the conditions in the upper tail, and the OTM European put options to the lower tail, in their risk-neutral distribution. If the distribution is symmetric, and the corresponding OTM call and put options have strikes exactly as far from the forward price as the other, then they must be priced equally. This is due to the fact that they have the exact same expected payoff. Hence, the discounted expected payoffs, option prices, must be equal. If the risk-neutral distribution has a positive skew, the OTM call option will be more expensive as it will be more likely to end up ITM than the corresponding OTM put option. The opposite is true when the distribution has a negative skew. Hence, the skewness premium of corresponding OTM call and put prices with strike price symmetrically around the forward price is a direct measure of the skewness of the risk-neutral distribution.

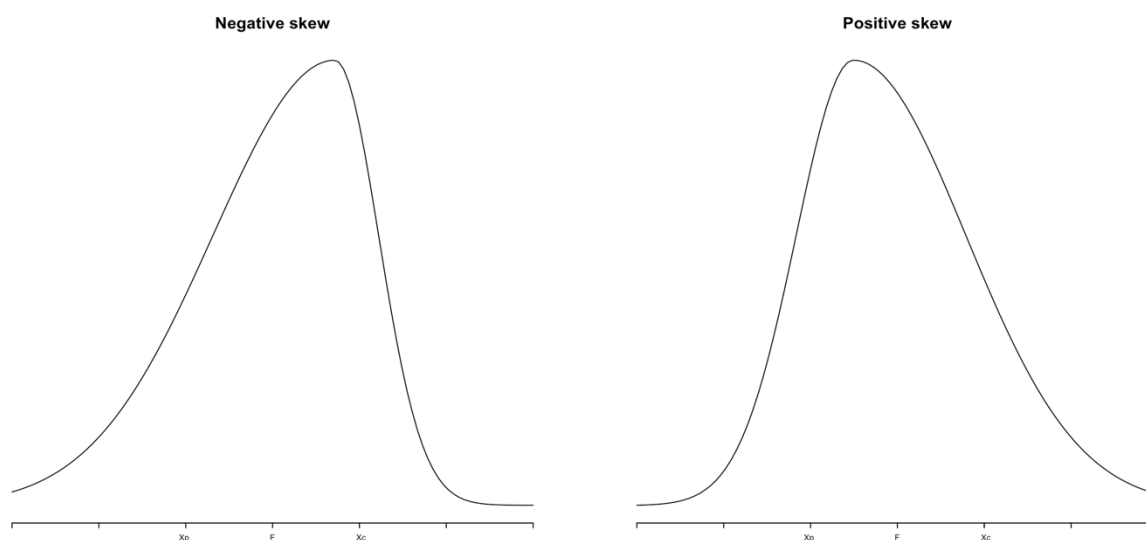


Figure 4. Risk-neutral distributions with positive and negative skewness. In the case of a positive skew, the probability of the call option ending up in-the-money at maturity is larger than for the corresponding put, hence the call should trade at a premium above the put price. The opposite is true for the distribution showing a negative skew.

Bates (1991) uses American options in his study due to the fact that the major exchange-traded options on market indexes at the time were American. The early exercise premium of American option prices over European option prices is determined by the optimality of early exercise. This optimality depends on the underlying assets cash flow primarily, while only secondarily on the distribution skewness. Hence, the direct effect of the risk-neutral distribution on the skewness premium does not hold for American options on the index. He thus uses American options on futures on the index. This solves the problem as the cost of

carry includes the effect of the cash flows on early exercise, and for futures the cost of carry is zero. Today, index options are typically European. By using European options, we avoid the problems due to early exercise and can use options directly on the index. Another benefit stems from the pricing of options. There was no known analytical solution for pricing American options on jump-diffusion processes, and Bates thus develops a quadratic approximation method. In contrast, pricing the European options is straightforward, as presented in Section 4.1.

Bates (1991) defines properties for the skewness premium that hold for the following distributional hypotheses; constant elasticity of variance (CEV) processes including special cases as the geometric and arithmetic Brownian motions, stochastic volatility processes and jump-diffusion processes. They hold for European options in general, American options on futures, and for all maturities. The properties are as follows (Bates, 1991, Proposition 1):

If $SK(x)$ lies between 0 % and x %, the market expectations can be interpreted as “neutral”, not implying any strong positive or negative expectations about the direction of the stock market. This holds for the standard distributional hypotheses:

- “standard” CEV processes and the special cases geometric and arithmetic Brownian motions. In the case of the geometric Brownian motion, $SK(x)$ would equal x %, while for the arithmetic Brownian motion it would equal 0 %.
- Benchmark stochastic volatility processes, where the volatility evolves independently of the asset price
- Benchmark jump diffusion processes; Merton’s (1976,a,b) specification of log-symmetric jumps with zero mean

If $SK(x)$ is negative, this may imply that the market participants are expecting negative jumps, hence the risk-neutral distribution has a negative skew. It may also imply that investors expect that if the market falls, the return volatility increases. If $SK(x)$ is larger than x %, this may imply expectations of positive jumps, hence the risk-neutral distribution has a positive skew. It may also imply expectations of an increase in the volatility of returns when the market rises. Table 3 summarizes the mentioned distributional hypotheses. It presents their actual stochastic process, as well as the corresponding risk-neutral process and implications for the skewness premium.

Hence, we can calculate the skewness premium during 2018 – 2020 and observe whether we find significant changes before and during the market crash. Next, we can use the above

discussion to draw inferences about the changes in market participants' expectations of negative jumps based on our results.

Actual Stochastic Process	Risk-neutral Process	Skewness Premium
<p>CEV processes</p> $dS = \mu S dt + \sigma S^\rho dZ$ <p>Special cases $\rho = 0$: arithmetic Brownian motion $\rho = 1$: geometric Brownian motion $0 < \rho < 1$: standard leverage effects</p>	$dS = bS dt + \sigma S^\rho dZ$	<p>SK < 0 only if $\rho < 0$</p> <p>$0 < \text{SK} < x\%$ if $0 < \rho < 1$</p> <p>SK > x% for $\rho > 1$</p>
<p>Stochastic volatility processes</p> $\frac{dS}{S} = \mu dt + \sigma_t dZ$ $d\sigma_t = \alpha(\sigma_t) dt + v(\sigma_t) dZ_\sigma$ $\text{Cov}(dZ, dZ_\sigma) = \rho_{s\sigma} dt$	$\frac{dS}{S} = b dt + \sigma_t dZ$ $d\sigma_t = [\alpha(\sigma_t) + \phi_\sigma] dt + v(\sigma_t) dZ_\sigma$ $\text{Cov}(dZ, dZ_\sigma) = \rho_{s\sigma} dt$ $\phi_\sigma \equiv \text{Cov}\left(\frac{dJ_w}{J_w}, d\sigma\right)$ <p>Standard Assumptions</p> <ol style="list-style-type: none"> Idiosyncratic volatility risk $\phi_\sigma = 0$ Or isoelastic utility, CRTS technologies $\phi_\sigma = \phi_\sigma(\sigma)$ 	<p>SK = x% for $\rho_{s\sigma} = 0$</p> <p>SK > x% for $\rho_{s\sigma} > 0$</p> <p>SK < X% for $\rho_{s\sigma} < 0$</p>

Jump-diffusion processes		
$\frac{dS}{S} = (\mu - \lambda E(\kappa))dt + \sigma dZ + \kappa dq$	$\frac{dS}{S} = (b - \lambda^* \bar{k}^*)dt + \sigma dZ + \kappa^* dq^*$	SK=x% for $\bar{k}^*=0$
$Prob(dq = 1) = \lambda dt$	$Prob(dq^* = 1) = \lambda^* dt$	SK>x% for $\bar{k}^* >0$
$1 + \kappa$ log-normally distributed	$\lambda^* = \lambda E \left[1 + \frac{\Delta J_w}{J_w} \right]$	SK<x% for $\bar{k}^* <0$
	$\bar{k}^* = E(\kappa) + \frac{Cov\left(k, \frac{\Delta J_w}{J_w}\right)}{E\left(1 + \frac{\Delta J_w}{J_w}\right)}$	
	<p>Standard Assumptions</p> <ol style="list-style-type: none"> 1. Idiosyncratic jump risk $\lambda^* = \lambda, \quad \bar{k}^* = E(\kappa)$ 2. Or isoelastic utility, CRTS technologies $1 + k^*$ log-normal; λ^* and \bar{k}^* constant 	
<p>Notation: Z and Z_σ = Wiener processes, J_w = the indirect marginal utility of optimally invested wealth for the representative investor, ΔJ_w = jump-contingent random change in J_w. The parameters of the jump diffusion processes are explained in Section 4.1. Note that the standard assumptions are not the only ones typically imposed, there are other restrictions required as restrictions on interest rate processes, frictionless markets, etc.</p>		

Table 3. Skewness premium under different classes of distributional hypotheses, from Bates (1991, p. 1017-1018).

3.2 Methodology

We wish to measure the daily skewness premiums of ATM and 4 % OTM options over time to see whether there is evidence of reactions in market expectations of negative jumps prior to the Covid-19 market crash. It follows from the discussion in Section 3.1 that under the mentioned distributional hypotheses, the ATM skewness premium should not differ much from the theoretical value of 0 %. We can use it to get an indication of the accuracy of the interpolation. The 4 % OTM skewness premium should vary between 0 – 4 % if the standard distributional hypotheses hold during the observed time period.

To calculate the ATM and OTM skewness premiums, we need the prices of puts and calls with strike prices equal to, as well as symmetrically around, the forward price. As this typically does not exist, we use cubic spline interpolation to estimate a relationship between the observed option prices (V), and strike prices (X), given the maturity (T). We use the cubic spline interpolation method, with certain restrictions discussed below, to ensure an estimated relationship consistent with theoretical considerations. No-arbitrage conditions and theoretical distributions imply that option prices are continuous, monotone and convex functions of the strike prices, (Bates, 1991).

A cubic smoothing spline is fitted through the observations of normalized strike prices, X_T/F_T , and corresponding normalized option prices, V_T/F_T . By normalizing the prices, we can easily find the estimated option prices we need based on their moneyness with all included maturities, from the estimated splines. The estimated V_T/F_T when $X_T/F_T = 1$ will thus equal the estimated ATM option price, as these options have strike price equal to the corresponding forward price. Put (call) options with X_T/F_T higher (lower) than 1 are ITM, and the opposite is true for the OTM options. The interpolation is done for each day, for puts and calls separately. In each interpolation, we use options with days until maturity between 28 and 118 days. This way, the estimated relationship between option price and strike price for each day takes into account more than one maturity.

From the estimated splines, we can calculate the daily skewness premiums using the estimated option prices for the desired strike prices:

$$\left(\frac{c_{T,X_c}}{F_T} / \frac{p_{T,X_p}}{F_T}\right) - 1 = \frac{c_{T,X_c}}{p_{T,X_p}} - 1$$

As discussed, for the ATM skewness premium, we use the estimated normalized option prices when X_T/F_T equals 1. Hence, when the strike price equals the forward price.

When calculating the 4 % OTM skewness premium, we use the estimated normalized option prices when $X_{T,c}/F_T = 1.04$ for calls and $X_{T,p}/F_T = 1/1.04$ for puts.

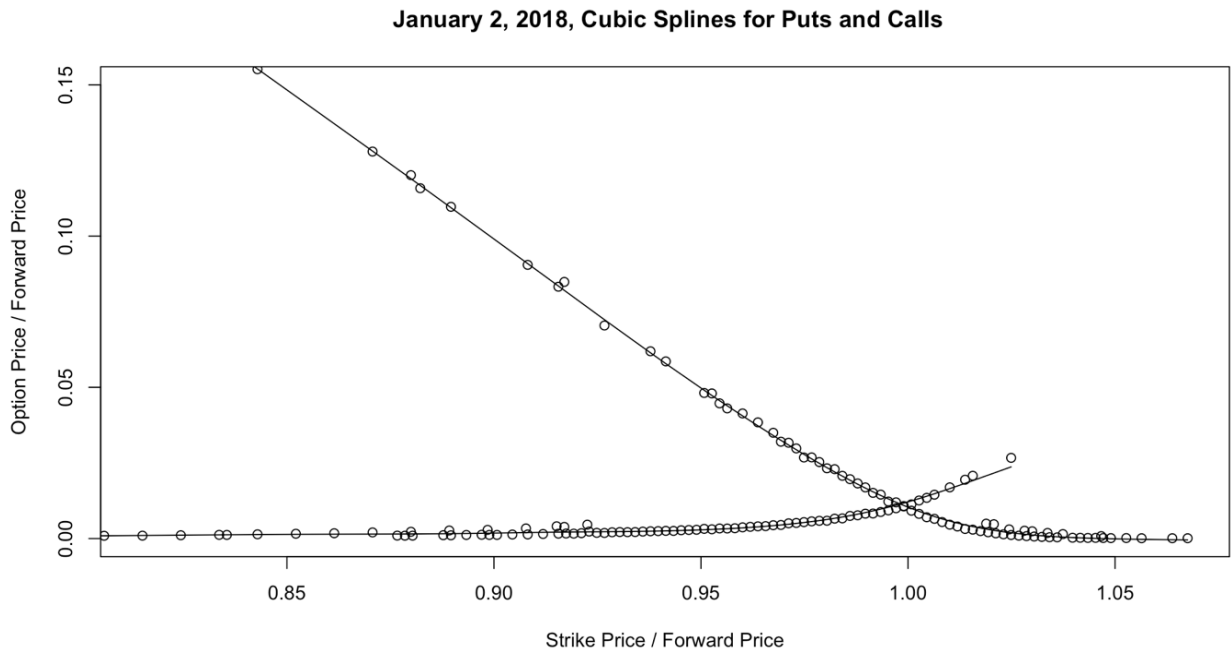


Figure 5. Estimated splines for puts and calls. An example of the estimated splines for the day January 2, 2018. Transaction prices divided by the forward price on the y-axis, and strike price divided by forward price on the x-axis. Cubic smooth splines is fitted through the observations, for calls and puts separately.

Figure 5 shows an example of the estimated splines of puts and calls for a specific day. From this we observe that the splines seem to fit the observations well, and that the splines of puts and calls cross when X_T/F_T is close to 1. This is consistent with the ATM skewness premium being close to 0.

During 2020, the variance of the observed prices increased by a large amount. Due to this, the degrees of freedom are adjusted to make the splines less sensitive. This is done to ensure that the option prices are a continuous, monotone and convex function of the strike prices. As using the same restriction on the degrees of freedom before 2020 leads to the splines not being a

good fit of the observed data, the imposed restrictions are different. Specifically, the degrees of freedom are set to 7 for 2018 and 2019, while 5 for 2020.

The inference from the estimated skewness premium is not affected by allowing the degrees of freedom to be set to 7 before 2020. In other words, the movement of the estimated V_T/F_T over time is not significantly different between splines with $df = 5$ relative to $df = 7$, when $X_T/F_T = 1$ for both options, 1.04 for calls and 0.96 for puts. The level is not affected much either, as the main effect on the splines from the difference in the restrictions is seen for the part covering ITM options ($\frac{X_T}{F_T} > 1$). Hence, the difference in the imposed restrictions makes the splines fit the observations well, ensures a continuous, monotone and convex relationship during the entire time period, but does not change the inference from the calculated skewness premium. Potential consequences of the restriction on the degrees of freedom are discussed further under Section 5.

As there are no available forward prices, synthetic forward prices are calculated assuming $F_{t,T} = S_t e^{(r-d)(T-t)}$. For each day we use forward prices with time to maturity ranging from 28 to 118 days, matched with the options of the same maturity. The quality of the synthetic forward price is not too important for our results, as the potential bias would be equal for all the calculated forward prices. We are not interested in the actual value of the forward price but rather the development in the relationship between V_T/F_T and X_T/F_T over time.

Figure 6 illustrates the daily mean standard errors of the fitted cubic splines. Specifically, the mean of the standard errors of the distance between observed prices and the cubic splines for calls and puts, each day. From this we observe that the standard errors get enormous during the market crash. They increase from the same day as the S&P 500 index begins to fall, February 20, 2020. The increased variance implies that market participants do not agree on the option prices, due to the increased uncertainty of the index price. Hence, market participants have different expectations of the future price movement of the S&P 500. By looking closer at the option prices each day during the market crash, we observe that the difference in prices for different maturities increase. The options of longer maturities become more expensive relative to the options of shorter maturities. This can be explained by increased volatility of the underlying price as well. As implied volatility in general increases option prices, it may imply that the longer the time horizon, the more uncertain the market participants are about the price movement of the index. Only a few days after July 23, when the S&P 500

index reaches its lowest value, the mean standard error of the splines return to normal levels. The relatively low standard errors observed during most of the time before the market crash can imply that the interpolation method is reliable during this time period.

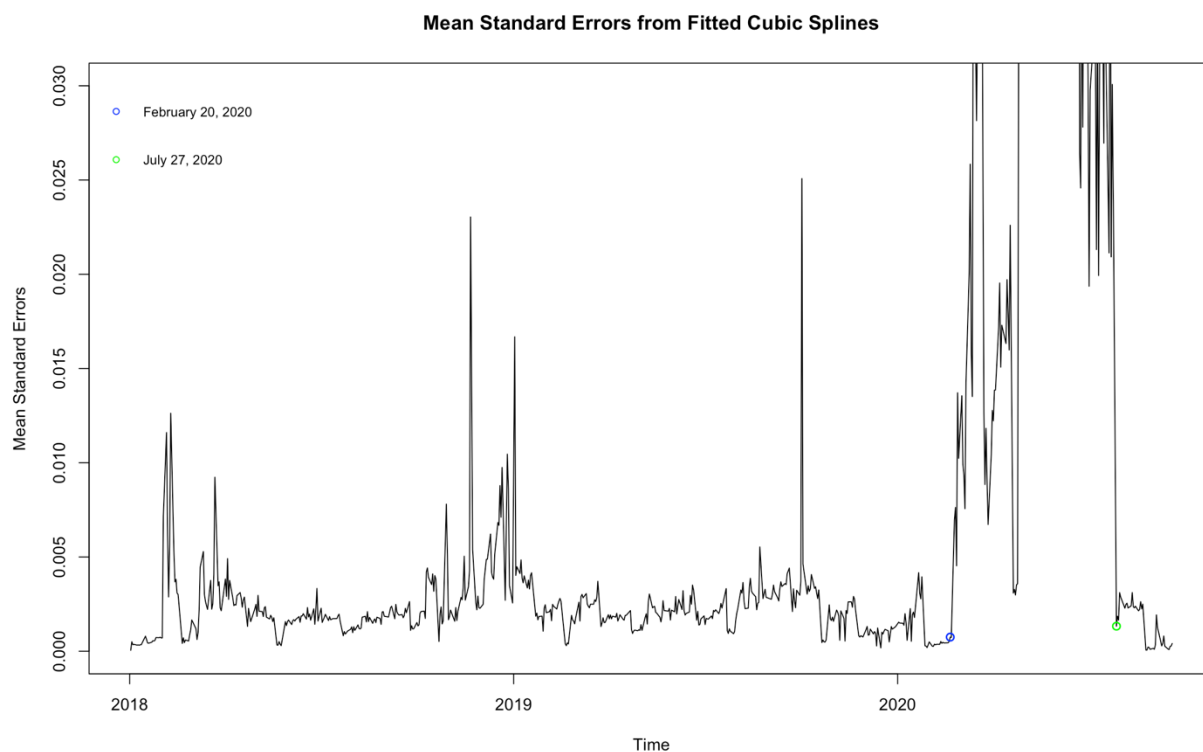


Figure 6. *The daily mean standard errors of the cubic spline interpolation of calls and puts. The standard errors increased a lot during the crisis. The blue dot marks February 20, 2020. After this day, the mean standard errors of the splines increased, implying disagreements on option prices, as well as higher difference in prices of options with different maturities. The green dot marks July 27, when the standard errors are back to normal levels (July 25 and 26 are missing from the dataset).*

3.3 Analysis

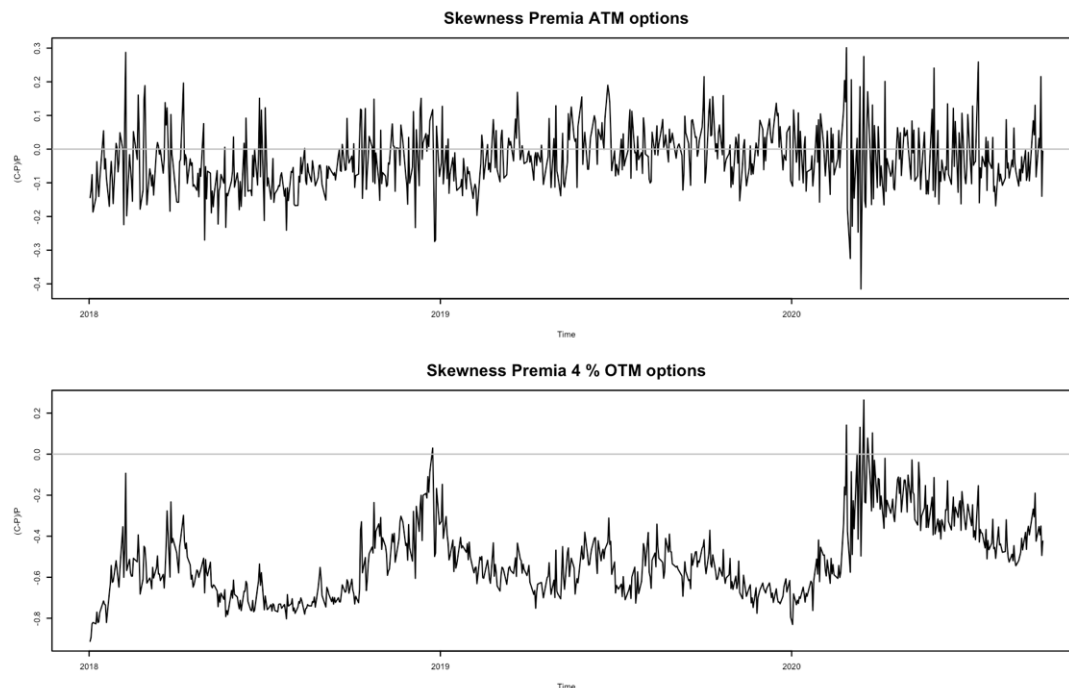


Figure 7. *The daily skewness premia of ATM and 4% OTM options. The skewness premia plotted over the time period January 2018 – October 2020. We use the 4 % OTM option skewness premium to make inferences about changes in market expectations. There is no evidence of reactions before February 20, 2020 (for zoomed plot see Figure 8 below). After this day, the skewness premium increases. On March 16, 2020, the skewness premium begins to decrease, implying that the market participants are buying protection.*

Figure 7 shows the graphs of the daily ATM and 4 % OTM skewness premiums from 01/2018 – 10/2020. We observe from the first graph that the skewness premium of the ATM options is varying around zero, but it has quite a large variance relative to the one measured in Bates (1991). For the distributional hypotheses mentioned, the ATM skewness premium should not deviate much from the theoretical value of 0 %. As observed in Figure 7, even though it varies around zero, the skewness premium does in fact deviate from 0 % by quite a large amount for the entire time period. It suggests that the interpolation method might not be reliable, or that the mentioned distributional hypotheses does not hold, which is discussed further in Section 5.

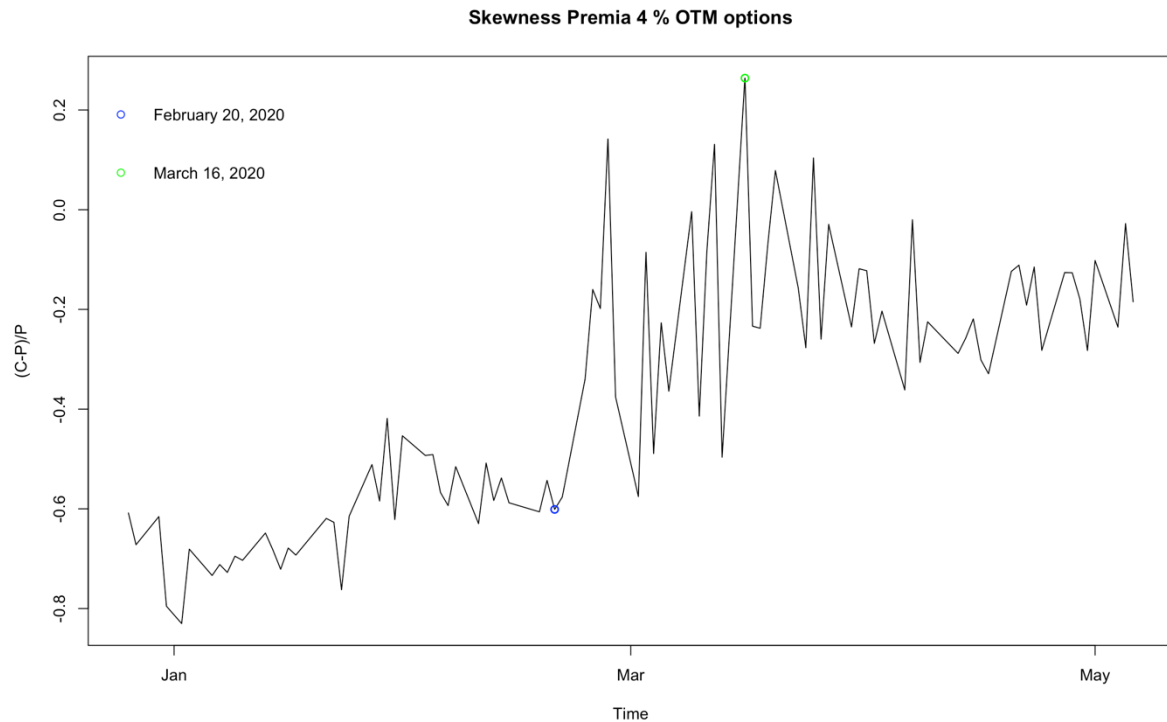


Figure 8. Zoomed plot of 4 % OTM options skewness premia, January–May 2020. Blue dot marks February 20, when we first observe reactions in the market as the skewness premium increases. The green dot marks March 16, when the skewness premium begins to fall. This implies that market participants are buying protection, as the 4 % OTM put options become more expensive relative to the corresponding 4 % OTM call option.

From the second graph of Figure 7 we observe that the 4 % OTM option skewness premium has been mostly negative for the observed time period, with a small exception at the end of 2018. As mentioned in Section 2, the reason why the put options are trading at a premium relative to the corresponding call options, may be due to a higher demand for puts. This is discussed further in Section 4.3.2. In Bates' study, the skewness premium begins to fall a year preceding the crash. It then returns to normal levels, before falling when the crash occurs. In contrast, we observe from Figure 8 that the skewness premium increases during the beginning of the crash, before decreasing from mid-March. We observe that it does not stay within the limits of 0-4 %, suggesting that the standard distributional hypotheses do not hold for the observed time period. As discussed, the negative OTM skewness premium suggests that the market participants either have expectations of negative jumps, or that the volatility of returns will increase in the case of a market fall.

Hence, we observe no evidence of changes in market expectations of jumps prior to February 20. These results are in line with the findings of Hanke, Kosolapova and Weissensteiner (2020), who use risk-neutral densities to measure market expectations regarding Covid-19. When the

index falls, we observe a reaction in the skewness premium as it becomes less negative. As the market participants fear a crash, the probability on the left side of the risk-neutral distribution, reflecting the low outcomes, increases. This fattens the left tail, resulting in a more symmetric distribution, (Jackwerth, 2020). Hence, the put options become less expensive relative to the call options. The increase reaches its peak on March 16, 2020, before decreasing, making the put options more expensive relative to the call options. This is a sign that market participants' crash fears increase, as they buy protection. Hence, the skewness premium shows a collapse of expectations in the middle of March. This is in line with the results of Kojien and Gormsen (2020) that use stock and dividend futures markets to investigate expectations, and Jackwerth (2020) using options on the S&P 500 index as well. It is also consistent with the findings of Ramelli and Wagner (2020), showing that in the beginning of the pandemic the stocks affected were the ones with strong exposure to China. They find that it was later on in the crisis that the market participants understood that a larger part of the stocks in the S&P 500 was affected as well.

As observed in the next part of the thesis, the result is consistent with the one obtained when extracting jump-parameters implicit in the SPX option prices.

4. Part 2: Option Pricing Under Asymmetric Jump-Diffusion Processes

In Section 4, we use Bates' option pricing model for asymmetric jump-diffusion processes to estimate the implicit jump-parameters in the observed option prices through optimization.

In Section 4.1, the theory behind pricing options under the jump-diffusion, the implicit jump parameters and how we will use them to draw inferences about market expectations is presented. In Section 4.2, we describe the procedure for estimating the implicit jump parameters, before an analysis of the results is presented in Section 4.3.

4.1 Theory

Bates' option pricing model is based on the proposition that the S&P 500 index follows a stochastic differential equation (SDE) with random jumps that may be asymmetric. The fact that they can be asymmetric is an important distinction from the work that was earlier done on jump-diffusion based option pricing. It had earlier been assumed to have a mean of zero. With a mean jump size greater than zero, the distribution is positively skewed relative to the geometric Brownian motion, while negatively in the case of a mean jump size less than zero. When the underlying follows the geometric Brownian motion, we obtain the following properties:

1. The underlying price is always larger than zero
2. The stock returns over non-overlapping time intervals are independent
3. The distribution of future stock returns is independent of past and present returns
4. It is Markov, meaning that all decision relevant information is contained in the current stock price

Bates' jump-diffusion mostly acts as the geometric Brownian motion, but it may jump discretely several times a year. The magnitude of the jump is random. The jump frequency follows a Poisson-distribution, while "1 + the random percentage jump amount" is log-normally distributed. Note that if the jump intensity is zero, the return dynamics would be identical to the ones in Black and Scholes (1973) and Merton (1973b).

The SDE is as follows (Bates, 1991, p. 1023):

$$\frac{dS}{S} = (\mu - \lambda E(\kappa) - d_t)dt + \sigma dZ + \kappa dq \quad (4)$$

, where:

μ = the instantaneous cum-dividend expected return on the S&P 500 index

d_t = the dividend yield of the S&P 500 index

σ = the instantaneous variance, conditional of no jumps

Z = a standard Brownian motion

κ = the random percentage jump amount, conditional on a Poisson-distributed event occurring

$$, E(\kappa) = e^\gamma - 1$$

$$, \ln(1 + \kappa) \sim N\left(\gamma - \frac{1}{2}\delta^2, \delta^2\right)$$

q = Poisson counter, with intensity λ

$$, \Pr(dq = 1) = \lambda dt$$

$$, \Pr(dq = 0) = 1 - \lambda dt$$

λ = Jump intensity parameter

From (4), dq is the standard Poisson jump counting process, with jump intensity λ that governs the frequency of jumps:

$$E(dq) = (\lambda dt)1 + (1 - \lambda dt)0 = \lambda dt.$$

where λ can be interpreted as the expected number of jumps in a time interval (Koehrsen, 2019). From Ross (2010) it follows that a stochastic process $[X(t), t \geq 0]$ is a compound Poisson process if it can be represented as:

$$X(t) = \sum_{i=1}^{N(t)} Y_i, t \geq 0$$

where $[Y_i, i \geq 1]$ is a sequence of independent and identically distributed random variables, and $[N_t, t \geq 0]$ is a Poisson process with intensity λ . The expected value of a compound Poisson process is calculated using the results known as Wald's equation ("Compound Poisson process", 2020):

$$E[X(t)] = E[Y_1 + \dots + Y_{N(t)}] = E[N(t)]E[Y_1] = E[N(t)]E[Y] = \lambda t E[Y]$$

In equation (4), κdq denotes the Poisson sum (Yan & Hanson, 2006):

$$\kappa dq = \sum_{i=1}^{dq} \kappa_i$$

As this is a compound Poisson process, it follows from the above definition that:

$$E(\kappa dq) = \lambda dt E(\kappa)$$

Over the time interval $[t, t + \Delta t]$, the expected value of the Poisson jump counting process is $\lambda \Delta t$. Hence, as time is measured in years, λ can be interpreted as the expected number of jumps per year (Tang, 2018). Over the time interval, the expected value of the compound Poisson process = $\lambda \Delta t E(\kappa)$. As time is measured in years, $\lambda E(\kappa)$ can be interpreted as the expected value of jumps per year, where $E(\kappa)$ is the mean jump size.

In Bates' model, there is another important distinction from the earlier work that was done on option pricing under jump-diffusions. Bates' risk-neutral jump diffusion is derived through restrictions set on the preferences of the representative investor and technologies. The reason being that the jump risk cannot be assumed to have a price of zero, as it would then need to be idiosyncratic meaning that it would be possible to diversify it away. The underlying of our study is the S&P 500 index, and for Bates the futures on this index, which is a wide stock index and known to be one of the best measures of large cap U.S. equities. Thus, it is not reasonable to argue its jump risk to be idiosyncratic. Instead, the restrictions imposed to derive the appropriate risk-neutral jump-diffusion in Bates (1991, p. 1024) are:

5. Frictionless markets
6. Optimally invested wealth of the investor follows a jump-diffusion:

$$\frac{dW}{W} = \left(\mu_w - \lambda E(\kappa_w) - \frac{C}{W} \right) dt + \sigma_w dZ_w + \kappa_w dq$$

, where:

- W = optimally invested wealth, C = consumption and μ_w is constant
- κ_w = the random percentage jump in wealth, conditional on the Poisson event occurring
- $\ln(1 + \kappa_w) \sim N(\gamma_w - \frac{1}{2} \delta_w^2, \delta_w^2)$
- $E(\kappa_w) = e^{\gamma_w} - 1$
- $Cov(\ln(1 + \kappa), \ln(1 + \kappa_w)) \equiv \delta_{sw}$

7. The representative consumer has time-separable power utility:

$$E_\tau = \int_\tau^\infty e^{-\rho\tau} U(C_\tau) d\tau$$

, where:

- $U(C) = \frac{C^{1-R}-1}{1-R}$

- R : relative risk aversion

Under these restrictions the jump risk is systematic and the instant riskless interest rate is constant. From this, Bates (1991, p. 1025) derives the risk-neutral jump diffusion as:

$$\frac{dS}{S} = (b - \lambda^* \bar{k}^*) dt + \sigma dZ + k^* dq^* \quad (5)$$

b = the cost of carry, in our case $r - d_t$

$$\lambda^* = \lambda E \left(1 + \frac{\Delta J_w}{J_w} \right) = \lambda e^{-R\gamma_w + \frac{1}{2}R(1+R)\delta_w^2}$$

, where $\frac{\Delta J_w}{J_w}$ is the jump in the marginal utility of wealth invested optimally

, R is the relative risk aversion of the representative investor

, and w is wealth.

$$\bar{k}^* = E(\kappa) + \frac{Cov\left(\kappa, \frac{\Delta J_w}{J_w}\right)}{E\left(1 + \frac{\Delta J_w}{J_w}\right)} = e^{\gamma - R\delta_{sw}} - 1 \equiv e^{\gamma^*} - 1$$

$$, \ln(1 + k^*) \sim N\left(\gamma^* - \frac{1}{2}\delta^2, \delta^2\right)$$

It follows from Bates (1991) that by extracting the risk-neutral jump-parameters, λ^* , \bar{k}^* , σ and δ , we can use them to calculate implied volatility and coefficients of skewness and kurtosis of the risk-neutral distribution of S_{t+T}/S_t . When observing the changes in the jump-parameters and the risk-neutral distribution over time, we can draw conclusions about the reactions of market expectations. When \bar{k}^* is equal to zero, (5) becomes the risk-neutral version of the geometric Brownian motion. Thus, the expected value of jumps per year, $\lambda^* \bar{k}^*$, is zero. The skewness premium of x % OTM options as measured in Part 1 would in this case be equal to x %. The expected value of jumps per year is positive when the mean jump size is greater than zero. The skewness premium is then higher than x %, and the distribution of S_{t+T}/S_t is positively skewed relative to the geometric Brownian motion. In the case of negative expected value of jumps per year, the mean jump size is below zero and the skewness premium of x % OTM options is less than x %. The distribution of S_{t+T}/S_t is negatively skewed relative to the geometric Brownian motion. When crash fears increase, the expected value of jumps per year become more negative relative to the case of weaker crash fears. This

is due to the expected number of jumps per year increasing, and the mean jump size becoming more negative.

In addition, we plot the VIX index during the observed time period to see whether it provides the same information about the expectations of jumps as the ones from our estimated jump-parameters. The VIX index is a popular measure for assessing the market risk and investors' sentiment, as it measures the expected volatility of the S&P 500 index over the next 30-days. In other words, it extracts the implied volatility from SPX option prices. Hence, we can use the VIX index as an indication of whether the movements of our estimated implied volatility are reliable. Likos (2020) describes the VIX index level. From this it follows that a VIX index level below 12 implies a reduced volatility, while a VIX index level over 20 is said to be high. A VIX index level in between 12 and 20 is considered to be normal. Hence, if the VIX increases, it indicates that the crash fears of the market participants become stronger. They become less confident in the market on a short term-basis.

From the formula of \bar{k}^* we can observe that the risk-neutral parameter is biased relative to the true parameter $E(\kappa)$. The bias depends upon the covariance between this jump amount and the jump in the marginal utility of the optimally invested wealth, divided by the expectation of $1 +$ the jump in marginal utility. As this covariance typically is negative, the implicit mean jump size typically has a downward bias.

From the risk-neutral jump diffusion, λ^* can also be interpreted as the cost of jump insurance per time unit. This is due to the process (5) being the specification of pure security prices given aggregate relative risk aversion, expressed as a jump-diffusion (Bates, 1991, p. 1025). Hence, the price at t of a pure security paying \$1 in the case that a jump appears between t and $t + \Delta t$, and \$0 otherwise, is $\lambda^* \Delta t$. In a risk-neutral world, the cost of such insurance is priced at the true fair rate, λ . Assuming that investors are risk averse, the cost would be higher than the true rate in the case of negative jumps, i.e., if $E(\kappa_w) < 0$, then $\lambda^* > \lambda$. Hence, the expected number of jumps per year we extract from the option prices will slightly overstate the true expected number of jumps per year, if the jumps have negative mean. Correspondingly, when we calculate the kurtosis and skewness of the underlying risk-neutral distribution using the implicit parameters, they will be slightly upward biased when jumps have negative mean. We see this from the following formulas for skew and kurtosis of the return distribution of the underlying (Bates, 1991, p.1024):

$$\text{Var}(S_{t+T}/S_t) = M_2 - (M_1)^2 \quad (6a)$$

$$\text{SKEW} = [M_3 - 3M_1M_2 + 2(M_1)^3]/(\text{Var})^{3/2} \quad (6b)$$

$$\text{KURT} = [M_4 - 4M_1M_3 + 6(M_1)^2M_2 - 3(M_1)^4]/(\text{Var})^2 \quad (6c)$$

, where:

$$M_n \stackrel{\text{def}}{=} E \left[\left(\frac{S_{t+T}}{S_t} \right)^n \right] = \exp \{ n(\mu - d - \lambda E(\kappa))T \\ + \left(\frac{1}{2} \right) (n^2 - n)\sigma^2T + \lambda T [e^{n\gamma + \frac{1}{2}(n^2-n)\delta^2} - 1] \}$$

Thus, the implicit mean jump size is typically downward biased, and in the case of negative mean jumps, the expected number of jumps per year as well as the skew and kurtosis of the return distribution is upward biased. With this said, given assumptions about the relative risk aversion and the degree to which total wealth is affected by the jumps in the index, the inference drawn from the changes in the risk-neutral parameters corresponds to the one of the true parameters. Bates (1991) shows this by making assumptions that the relative risk aversion is 2 (the Samuelson presumption), that equity comprises half of wealth and that jumps occur only in stock prices. Then, we have that (Bates, 1991, p. 1034):

$$\delta_{sw} \approx (\delta) \left(\frac{1}{2} \delta \right) = \frac{1}{2} \delta^2 \\ \lambda^* = \lambda e^{-2\left(\frac{1}{2}\gamma\right) + \frac{1}{2}R(1+R)\left(\frac{1}{2}\delta^2\right)} \approx \lambda e^{-\gamma} \\ \gamma^* = \gamma - 2 \left(\delta \left(\frac{1}{2} \delta \right) \right) \approx \gamma$$

given that the estimates of δ^2 are ≤ 0.005 .

Hence, if the true parameters increase (decrease), the risk-neutral parameters increase (decrease) as well. The inferences we draw from our analysis in Section 4.3 of the changes in the implicit risk-neutral jump-parameters over time thus apply to the true parameters, as the true parameters change in the corresponding direction.

We elicit the risk-neutral parameters from the SPX option prices. To obtain the price equations of the options from the risk-neutral jump diffusion, we adjust the price equations of European options on futures (Bates, 1991, p. 1026). By changing the underlying price from the futures price to the S&P 500 price, and using $b = r - d_t$ instead of $b = 0$, we obtain:

$$\begin{aligned}
c(S_t, T; X_c) &= e^{-rT} \sum_{n=0}^{\infty} \Pr * (n \text{ jumps}) E_t^*(\max(S_{t+T} - X_c, 0) | n \text{ jumps}) \\
&= e^{-rT} \sum_{n=0}^{\infty} [e^{-\lambda^* T} (\lambda^* T)^n / n!] [S_t e^{b(n)T} N(d_{1n}) - X_c N(d_{2n})]
\end{aligned} \tag{7a}$$

$$\begin{aligned}
p(S_t, T; X_p) &= e^{-rT} \sum_{n=0}^{\infty} \Pr * (n \text{ jumps}) E_t^*(\max(X_p - S_{t+T}, 0) | n \text{ jumps}) \\
&= e^{-rT} \sum_{n=0}^{\infty} [e^{-\lambda^* T} (\lambda^* T)^n / n!] [X_p N(-d_{2n}) - S_t e^{b(n)T} N(-d_{1n})]
\end{aligned} \tag{7b}$$

, where:

$$\begin{aligned}
b(n) &= (r - d_t - \lambda^* \bar{k}^*) + \frac{n\gamma^*}{T} \\
d_{1n} &= \frac{[\ln(\frac{S_t}{X}) + b(n)T + \frac{1}{2}(\sigma^2 T + n\delta^2)]}{\sqrt{(\sigma^2 T + n\delta^2)}} \\
d_{2n} &= d_{1n} - \sqrt{(\sigma^2 T + n\delta^2)}
\end{aligned}$$

and T is time to maturity measured in years.

Hence, we use Bates' option pricing model for asymmetric jump-diffusion processes to estimate the implicit jump parameters in the observed option prices. From these, we calculate the implied variance, and coefficients of skewness and kurtosis of the risk-neutral return distribution of the S&P 500 index. Then, we observe them over time to see whether we find evidence of reactions in the estimated parameters before the market crash began. We use the above discussion to draw inferences about what the results imply for market participants' expectations of negative jumps.

4.2 Methodology

We now proceed to describe how we estimate the unknown jump-parameters λ^* , \bar{k}^* , σ and δ . This section contains details of the additional sample restrictions, followed by a description of the estimation model and the approach for calculating the skewness, kurtosis and the implied volatility.

4.2.1 Sample Restrictions

We make additional restrictions on the dataset introduced in Section 2. Only options that start and expire within the range of 28-118 days are included. Then, 20 calls and 20 puts are chosen for each day in the estimation. The reason for the restrictions is to set a finite limit on the total number of options included in the estimation, to avoid overabundance of data and to speed up the estimation time. Whether this can create biased estimates is discussed in Section 5. The total number of call and put options in the sample is respectively 4470 and 5825.

4.2.2 Estimation Model

Similar to the study of Bates, the normalized option prices on one particular day are assumed to be the normalized theoretical price, plus an error term (Bates ,1991, p.1027-1030):

$$\frac{V_i}{F_t} = \frac{V(S_t, T; X_i, \lambda^*, \bar{k}^*, \sigma, \delta)}{F_t} + \epsilon_i \quad (8)$$

where $V = c$ or p , $i = 1, 2, 3 \dots N$, and N is the total daily number of calls and puts each, which is set to 20. We choose the option prices based on the total number of prices quoted with the same T within one day and the strike price (X). We allow for only one T each day, but the chosen T can vary across days. First, we choose the T for each day, based on the number of options available with the same maturities. Then, we choose 20 calls and 20 puts based on the strike price, to spread the moneyness as much as possible for the options of the chosen T . The forward price F is a synthetic forward as described in Section 3.2. To estimate the jump-parameters implicit in the option prices each day, we optimize over the residual sum of squares (RSS). The RSS can be defined as:

$$\psi_V(\lambda^*, \bar{k}^*, \sigma, \delta) = \sum_{i=1}^{N=20} \left(\frac{V_i^M - V_i}{F} \right)^2 \quad (9)$$

Thus, the RSS can be seen as a measure of how well the theoretical prices V_i fit the market prices V_i^M . To minimize the sum of RSS for calls and RSS for puts as shown in (10) is therefore a way to estimate the jump-parameters that fit the market prices best. The optimization problem with the associated constraints on the parameters can then be defined as:

$$\begin{aligned} \min_{\lambda^*, \gamma^*, \sigma, \delta} (\psi_c(\lambda^*, \gamma^*, \sigma, \delta) + \psi_p(\lambda^*, \gamma^*, \sigma, \delta)) \quad (10) \\ 0 \leq \lambda^* < \infty \\ -\infty < \gamma^* \leq \ln(2) \\ 0 \leq \sigma \leq 1 \\ 0 \leq \delta \leq 1 \end{aligned}$$

where the average risk-neutral mean jump size \bar{k}^* is calculated¹ from estimating the jump parameter γ^* . Minimizing the sum of RSS for calls and RSS for puts as in (10) is a simple way to combine the theoretical price formulas for put and calls into one estimation problem. We use the function *nlinb* from R's *stats* package (R Core Team, 2020, p.1526) to estimate the parameters for each day in the period. This function minimizes the objective function (10) by default and allows for upper and lower bounds on the parameters.

One of the strengths of applying the *nlinb* function to the estimation problem is that it always converges to a solution and is faster in computational time, relative to other functions for constrained optimization in R, like the function *optim* (R Core Team, 2020, p.1544). The favourable solutions-messages from the optimization problem using *nlinb* are denoted in R, and defined by Gay (1990, p.5) as a) X-convergence, b) relative function convergence, c) both X- and relative function convergence and d) absolute function convergence. One of the downsides with the function is that it searches for local optima, and finds the best solution based on the stopping tolerances and start-values for the parameters we wish to estimate, which must be stated (Gay, 1990, p.7). The global/local optimum solution is defined by Solver (n.d.),

¹by the relationship: $\bar{k}^* \stackrel{\text{def}}{=} e^{\gamma^*} - 1$

where the global optimum solution is defined as “the one where there are no other feasible solutions with better objective function values”. The local optimum solution is defined as “the one where there are no other feasible solutions “in the vicinity” with better objective function values”. The global optimum solution is preferred since it is the maximum/minimum of the possibility space.

When executing the minimization problem multiple times within the same day with different start-values (all else being equal), the objective function converges to different solutions for the parameters each time denoted with the favourable solutions-messages. This is an indicator that there are many local minima in the objective function (10), making it very sensitive to the start values that must be stated in order to run the function *nlinb*. A working paper from Gili and Schumann from 2010 states that:

Many optimization problems in finance and economics have multiple local optima or discontinuities in their objective functions. In such cases it is stressed that ‘good starting points are important’. (..). We find that while ‘good starting values’ suggested in the literature produce parameters that are indeed ‘good’, a simple best-of-N-restarts strategy with random starting points gives results that are never worse, but better in many cases. (p. 1)

Since the solutions from multiple estimations were different within one day, we use the best-of-200-restarts method with random start-parameters each time. Hence, within each day, we set the total number of estimations to 200. The final parameters selected from these estimations are the ones that minimize the objective function (10) the most.

When estimating parameters for each day in the time period, there are some solutions for the jump parameters that are denoted with false convergence or other non-favorable messages. A total of 13 days² are removed from the final solutions data, based on non-favorable convergences messages. In addition, one day³ is removed due to a low number of option prices. As there are 10 days at the end of September and the beginning of October 2020 with a low number of option prices as well, our analysis is done for the time interval January 2018 – September 18, 2020. The days we remove are relatively spread across the estimation period, with exception of 23rd-24th of March 2020. On the 23rd of March, the S&P 500 reached its

² 2018-10-22, 2018-11-12, 2019-03-25, 2019-04-22, 2019-08-12, 2020-02-27, 2020-03-06, 2020-03-23, 2020-03-24, 2020-04-22, 2020-06-11, 2020-07-28 and 2020-07-30

³ 2020-01-29

lowest point. This might affect our analysis in that we are not able to extract the expectations from the option prices on that day. But overall, we will still be able to analyze whether there is evidence of a *change* in investors' expectations before and during the crash. Other than this, there is nothing special of relevance happening on the removed days.

The time used to estimate the jump-parameters within one day is approximately 7 minutes, which is the reason to only use 20 prices of puts and 20 prices of calls each day. As Gili and Schumann (2010, p. 5) states; there is a tradeoff between the quality of the solution and how much computing time one can afford. In this case, we find the computational time of 7 minutes per day necessary to get the most reliable solution with the available computing time.

A weakness of the best-of-200-restarts method is that we cannot be sure that the best solution out of the 200 estimations on one day is truly the global minimum. Discussed below are some important aspects regarding how “good” the random start-parameters are, and if the construction of the stopping tolerances is right. In Table 4 below we can observe that different combinations of the jump-parameters can result in almost identical theoretical option prices, when testing for different values of the parameters manually.

Theoretical Option Values Under Assymmetric Jump diffusion Process					
S=3500, X=3200, r=0.0065, d=0.0165, T=0.25					
Input				Output	
λ	γ	σ	δ	Call	Put
0.000	0.00000	0.14140	0.0000000	303.1698	12.38176
0.673	0.20617	0.10000	0.1000000	303.1694	12.38140
10.000	0.00000	0.10011	0.0311737	303.1695	12.38151

Table 4. Theoretical option prices. Different combinations of jump-parameters which can yield approximately the same price for both calls and puts.

Regarding the random start-parameters, the function *runif* from R's *stats* package (R Core Team, 2020, p.1729) is used to create random numbers within the bounds of each parameter. This function creates random numbers from the uniform distribution for each parameter. Thus, there is equal probability for every number to be selected within each of the parameters bounds.

An example of 200 generations of random combinations of start-parameters for σ , δ and γ^* can be seen in Figure 9. As seen in the figure, the different combinations of the start-parameters are relatively evenly spread across the axes. When adding more unknowns in the estimation problem, the total number of possible combinations of start-parameters increases. If we assume that there are for example 21 possible start-parameter values each for σ , δ and γ^* , the total number of possible combinations of the start-parameters would be 9261. If we assume that there are in addition 150 combinations of λ^* , the total possible combinations of the four start-parameters would become 1 389 150. Hence, there are in practice several million possible combinations of the four start-parameters, and the possibilities of getting the “right combinations” must be seen in combination with the fact that the total number of local optima is unknown. When executing the best-of-200-restarts method multiple times within a random day with random start-parameters (all-else being equal); the value of the objective function and the parameters chosen for the solution was the same each time. Hence, the random start-parameter method using *runif* is used in the estimation.

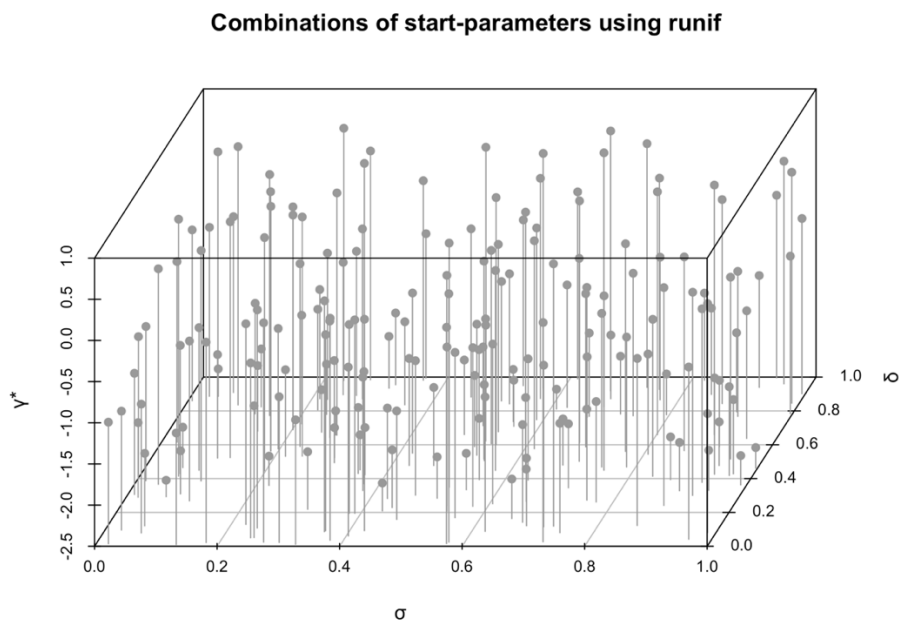


Figure 9. Random combinations of start-parameters. The Random combinations of the jump-parameters σ , δ and γ^* are evenly spread in the admissible domain.

Regarding the construction of the stopping tolerances in *nlsminb*, the maximum number of iterations allowed is 500. This is the total number of steps allowed that the function *nlsminb* can take to find the minimum. The step size is set to minimum 1 and maximum 70. The maximum possible number of evaluations of the objective function is set to 300 and the

absolute tolerance is set to zero. According to Gay (1990), an absolute tolerance of zero while receiving the convergence-message “absolute function convergence” would mean a perfect fit between the market prices and the theoretical prices. Other control parameters are set to default, like the relative tolerance and the X tolerance. Relative tolerance and X tolerance are measures of tolerable distances between the theoretical prices and the market prices, only calculated differently (Gay, 1990, p.7). Since the number of evaluations and iterations are higher than default and the other tolerances are the same as the default settings, there is no indication why these settings would not be correct. From running test-estimations of the best-of-200-restarts method on different days, we found that dividing by F in the formula for RSS in equation (9) for each option did not change the estimated parameters. This indicates that the tolerances are not influenced by whether we divide on F or not.

4.2.3 Implied Volatility, Skewness and Kurtosis

As discussed in Section 4.1, we use the estimated jump-parameters to calculate the implied variance and coefficients of skewness and kurtosis implicit in the option prices, from equation (6a-c). As the implied volatility is the standard error of the underlying return distribution, it equals the square root of the implied variance:

$$Vol\left(\frac{S_{t+T}}{S_t}\right) = \sqrt{Var\left(\frac{S_{t+T}}{S_t}\right)}$$

From the discussions in Section 4.1 and Section 3.1, it follows that we can make inferences about the changes in investors’ expectations of jumps by observing the changes in the above measures. The implied volatility, and coefficients of skewness and kurtosis of the underlying risk-neutral return distribution are calculated for each day and plotted over time in Section 4.3.2. In addition, we plot the value of the VIX index over time to observe whether it captures the same information about the market expectations of jumps, as discussed in Section 4.1.

4.3 Analysis

The results from the estimation are presented in this section. First, we analyse the estimated jump-parameters before we proceed with the skewness and kurtosis, the implied volatility as well as the VIX index.

4.3.1 The Estimated Jump Parameters

Figure 10 – 14 show the estimated jump parameters λ^* , \bar{k}^* and δ in the period from January 2018 to September 2020.

From Figure 10 we observe that the estimated expected number of jumps per year, λ^* , is relatively low during the entire period as opposed to the results from Bates (1991). We observe that in times after larger drops in the S&P 500, it tends to increase by a relatively large amount. This is the case in the period after the index price fall during the end of 2018, as well as during the Covid-19 crash. The reaction to the Covid-19 market crash seem to appear in mid-March, when the expected number of jumps per year increases and reaches its peak on March 16, 2020. The estimated average jump size, \bar{k}^* can be seen in Figure 12. From this we observe that it fluctuates around -15 % during most of the observed time period. We can also observe that it tends to take on larger negative values in time periods after the drops in the S&P 500 mentioned above. The estimated average jump size also seems to react to the Covid-19 market crash in mid-March, when it becomes strongly negative. Figure 13 shows the expected value of jumps per year, $\bar{k}^*\lambda^*$, which is negative during most of the observed time period. From the discussion above it follows that the expected value of jumps per year should become largely negative in the period after a fall in the S&P 500. We observe from Figure 13 and Figure 14 that this happens in mid-March. Hence, the market participants now expect larger negative jumps than before. We can also observe from Figure 13 that after the first negative reaction of a market fall, the expected value of jumps per year tend to increase to larger, positive values. This is the case after the S&P 500 drop at the end of 2018 and is also the case after the Covid-19 crash. In April 2020, the expected value of jumps per year become positive, before returning to negative levels. It fluctuates a lot due to the large uncertainty about the future value of the S&P 500. There is large uncertainty about the further development of Covid-19 and the future economic consequences. This is also seen in the implicit jump standard

deviation, δ . Figure 11 indicates that during the drops in the S&P 500, the jump volatility increases. It is relatively steady in the period from March 2019 until March 2020. During March 2020, the jump standard deviation peaks over 75% and during April it peaks to 100%.

Hence, we observe that there is no sign of changes in investors' expectations prior to the Covid-19 market crash. It is not until March 2020, that the estimated parameters seem to fully react to the crisis. Thus, the expectations of jumps do not seem to change until a while after the S&P 500 begins to fall.

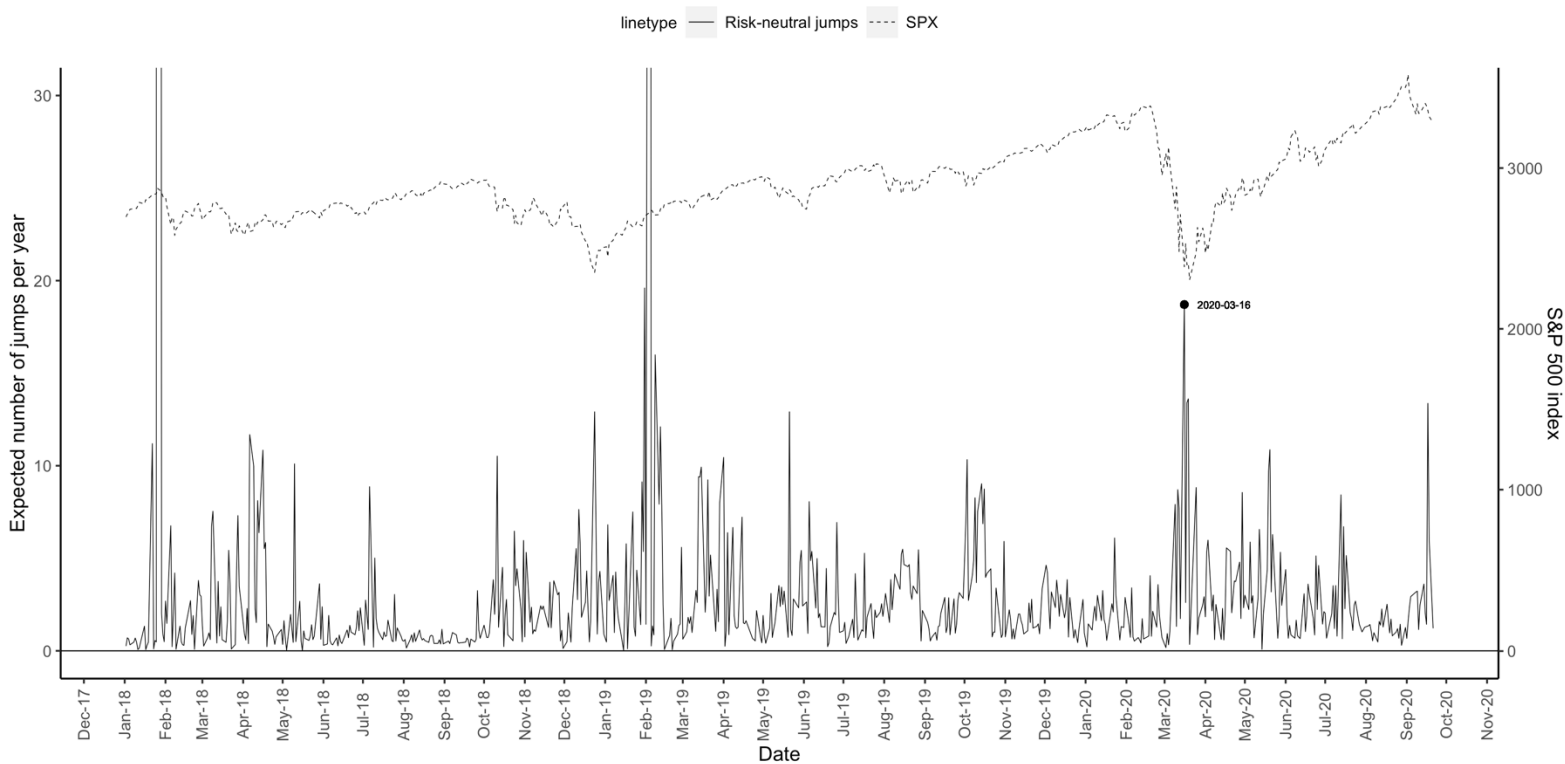


Figure 10. Risk-neutral expected number of jumps per year and the price of the S&P500.

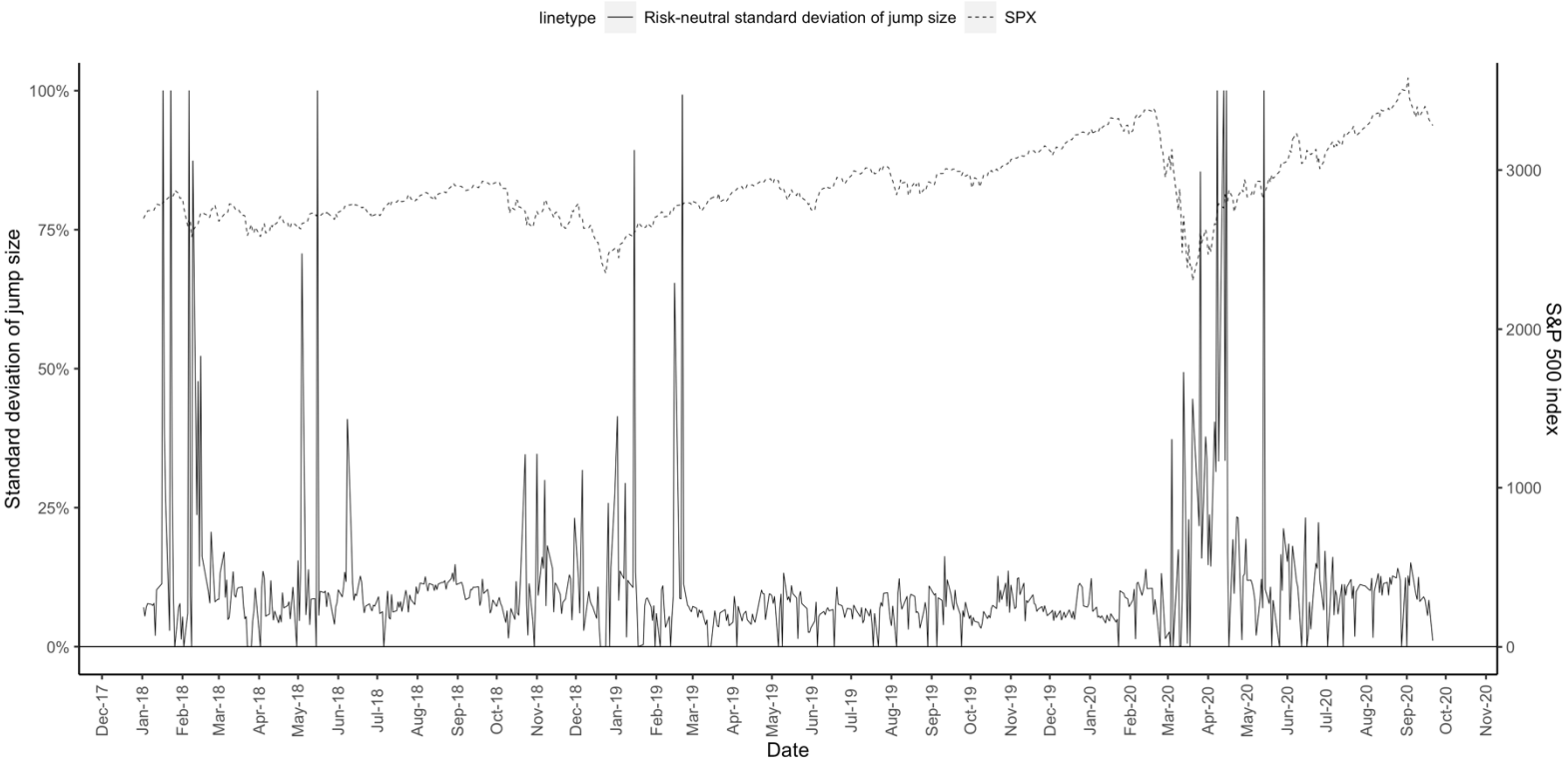


Figure 11. Implicit jump standard deviation of jump size and the S&P 500 index.

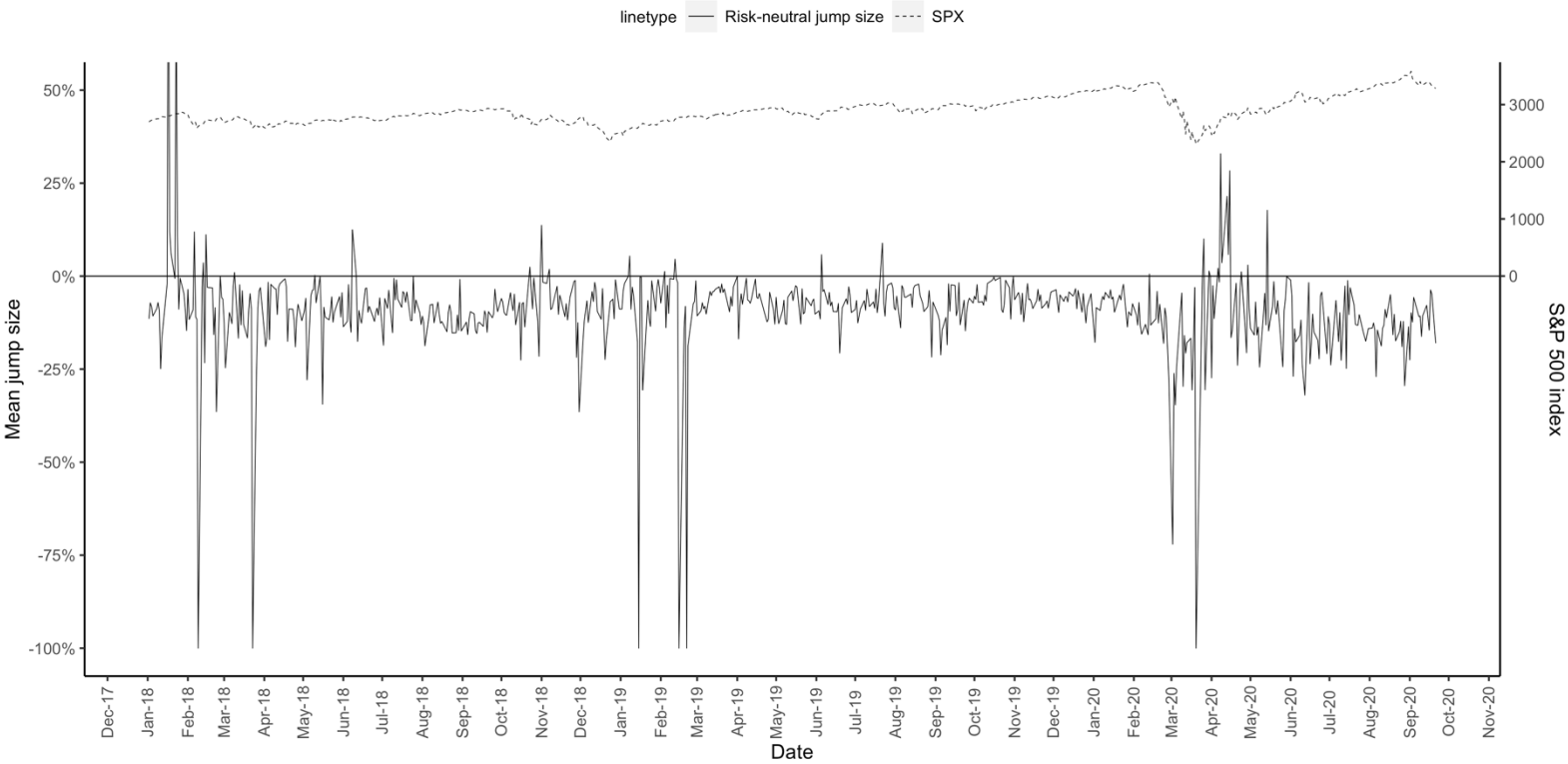


Figure 12. The risk-neutral mean jump size (conditional on a jump) and the SPX.

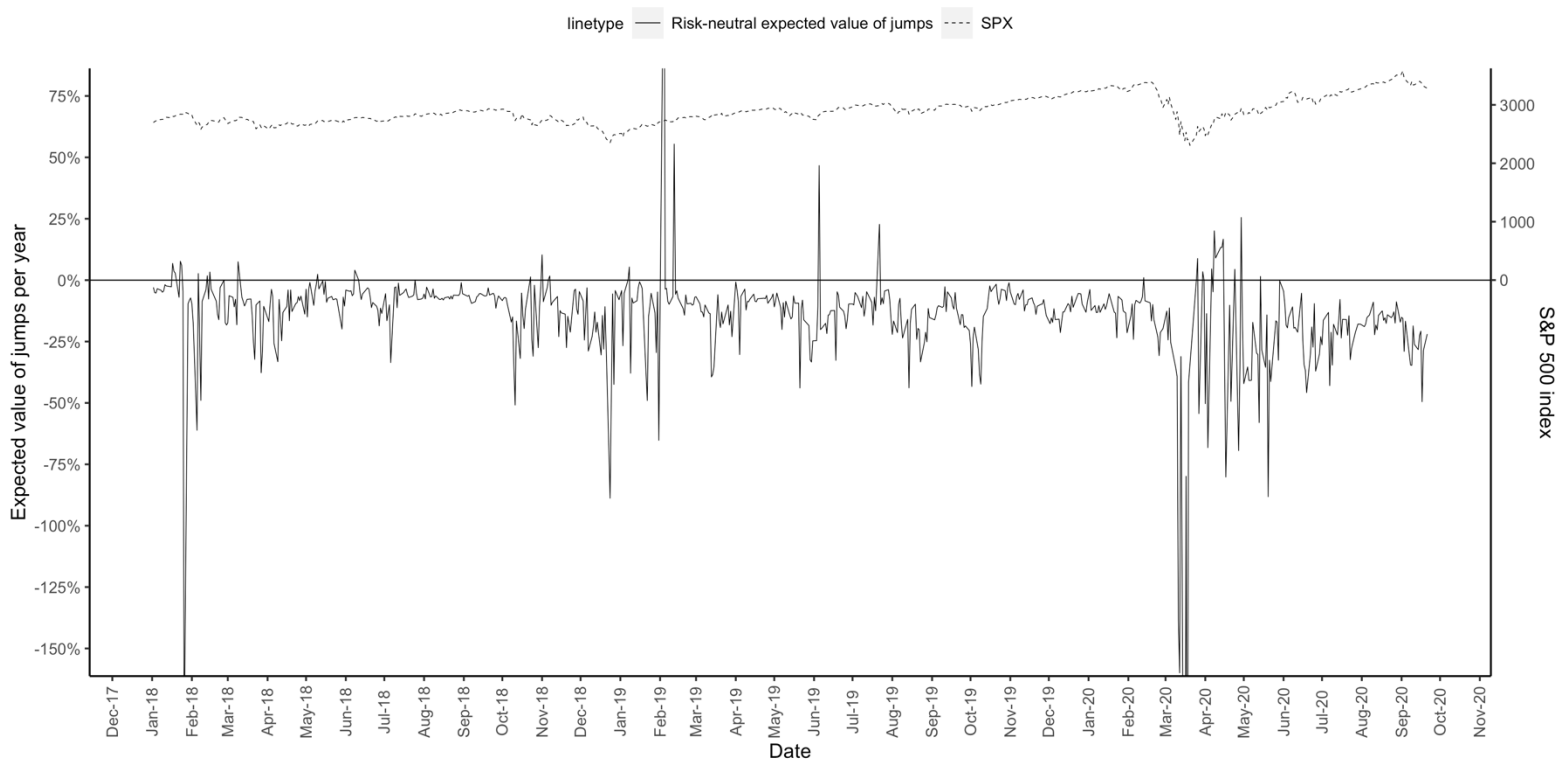


Figure 13. The risk-neutral expected value of jumps per year and the S&P 500 index.

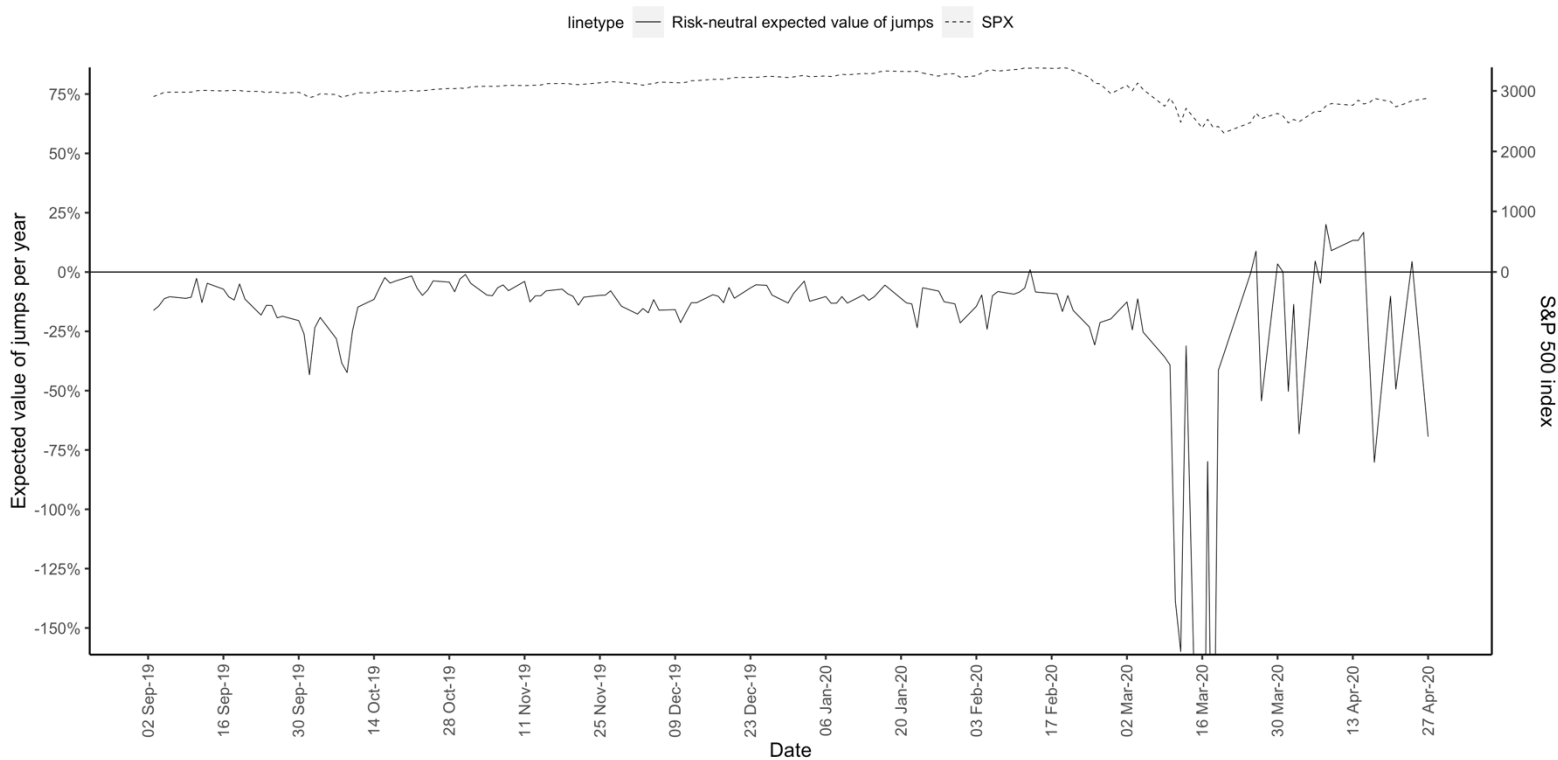


Figure 14. The risk-neutral expected value of jumps per year, zoomed.

4.3.2 Implied Volatility, Skewness and Kurtosis

The results of the calculated implied volatility, skewness and kurtosis implicit in the option prices based on risk-neutral probabilities can be seen in Figure 15-18. The skewness plotted over time in Figure 15 indicates that the underlying risk-neutral return distributions of the index was mostly negatively skewed during the examined time period. It follows from the discussion in Section 4.1 that this is explained by the implicit average jump size from Figure 12 being mostly below zero. The skewness becomes less negative during the beginning of the crisis, which is consistent with the findings in Part 1 and discussed in Section 3.3.

We observe that the skewness does not seem to decrease until the end of April 2020. Figure 17 shows the calculated kurtosis over the observed time period. It increases from March 2020, implying that the risk-neutral return distribution of the S&P 500 becomes more pointed around its mean.

A distinction from the method used in Bates (1991) is that he used the interpolated prices to obtain the implicit jump parameters, whereas we have used the true market transaction prices of the options. This is due to the fact that we used several maturities in the interpolation to observe the skewness premium reflecting expectations from more than one maturity. In this part on the other hand, we reduce the noise by using one maturity each day.

As opposed to the skewness Bates (1991) found in his study, which was mostly positive, our result shows negative skewness during most of the period of the estimation. This is an interesting result. As discussed in Part 1, it can indicate that the market either expects negative jumps during most of the observed time period or that the volatility will increase in the case of a crash. Covid-19 did not break out until December 2020, and the skewness and expected value of jumps showed no reaction in December nor in January as discussed above. The skewness, and the skewness premium calculated in Part 1, being negative during most of the observed time period may be explained by a higher demand for puts than for calls. It is possible that this is a consequence of historical stock market crashes, leading to investors wanting to protect themselves from the possibility of a large market fall. After the crash of 87, the puts became more attractive and are still more expensive relative to calls (Wolfinger, 2020). This could either imply that there are fewer sellers of puts in the market relative to buyers, or that the demand is higher for puts. In Section 2 we found that the total open interest each day was higher for puts than for calls from January 2018 to October 2020, and that it was about the same number of calls as puts. This suggest that the put options are trading at a premium relative

to the call options due to a higher demand for puts. Wolfinger (2020) states that “There currently exists a number of investors (and money managers) who never again want to encounter a bear market while unprotected, i.e., without owning some put options. That results in continued demand for puts”. Another possibility for why puts are trading at a premium relative to the call options, is the record long bull run in the stock market prior to the Covid-19 crash, starting in 2009. A high market may make investors worry about a correction, thus increasing the demand for put options as a protection of a possible market fall.

Figure 18 shows the implied volatility. We observe that it begins to increase in March 2020. Hence, the expected uncertainty about the future values of the S&P 500 price increases. During March, the implied volatility increases to over 50% before it peaks over 60% in April. Before March 2020, the implied volatility shows no evidence of increasing crash fears as it is relatively steady during the whole period from March 2019 to February 2020. This is consistent with the already discussed result that the full impact of the crisis is not observed in the market participants’ expectations of jumps until mid-March. As we observe from Figure 18, the implied volatility calculated moves similar to the VIX over time, suggesting that our estimate is reliable during this time period. The VIX begins to increase in March as well and takes on values higher than 20. As discussed in Section 4.1, this suggests a high level of expected fluctuations in the S&P 500 index over the next 30 days. Hence, the changes in the VIX index also indicate that the crash fears of the market participants begin to increase in March.

Thus, from the changes in the coefficients of skewness and kurtosis of the risk-neutral return distribution of the S&P 500, as well as the implied volatility and the VIX index, there is no evidence of increasing crash fears prior to the Covid-19 crash. Again, our estimates suggest that the crash fears begin to increase in March 2020.

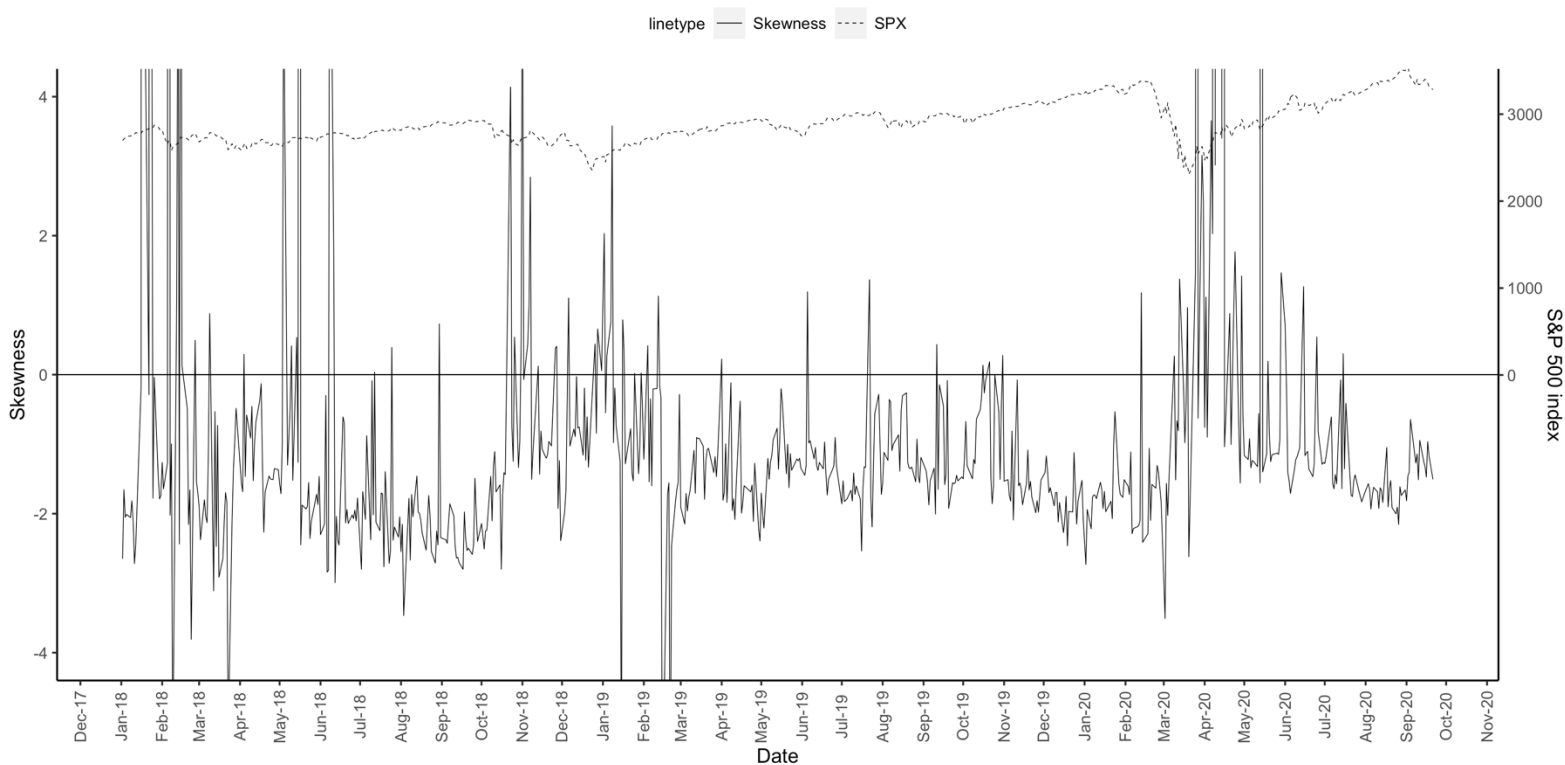


Figure 15. The implicit skewness of the risk-neutral distribution of the S&P 500 index. We observe a general level of negative skewness during the estimation period. It becomes less positive in the beginning of the crisis, before decreasing in April.

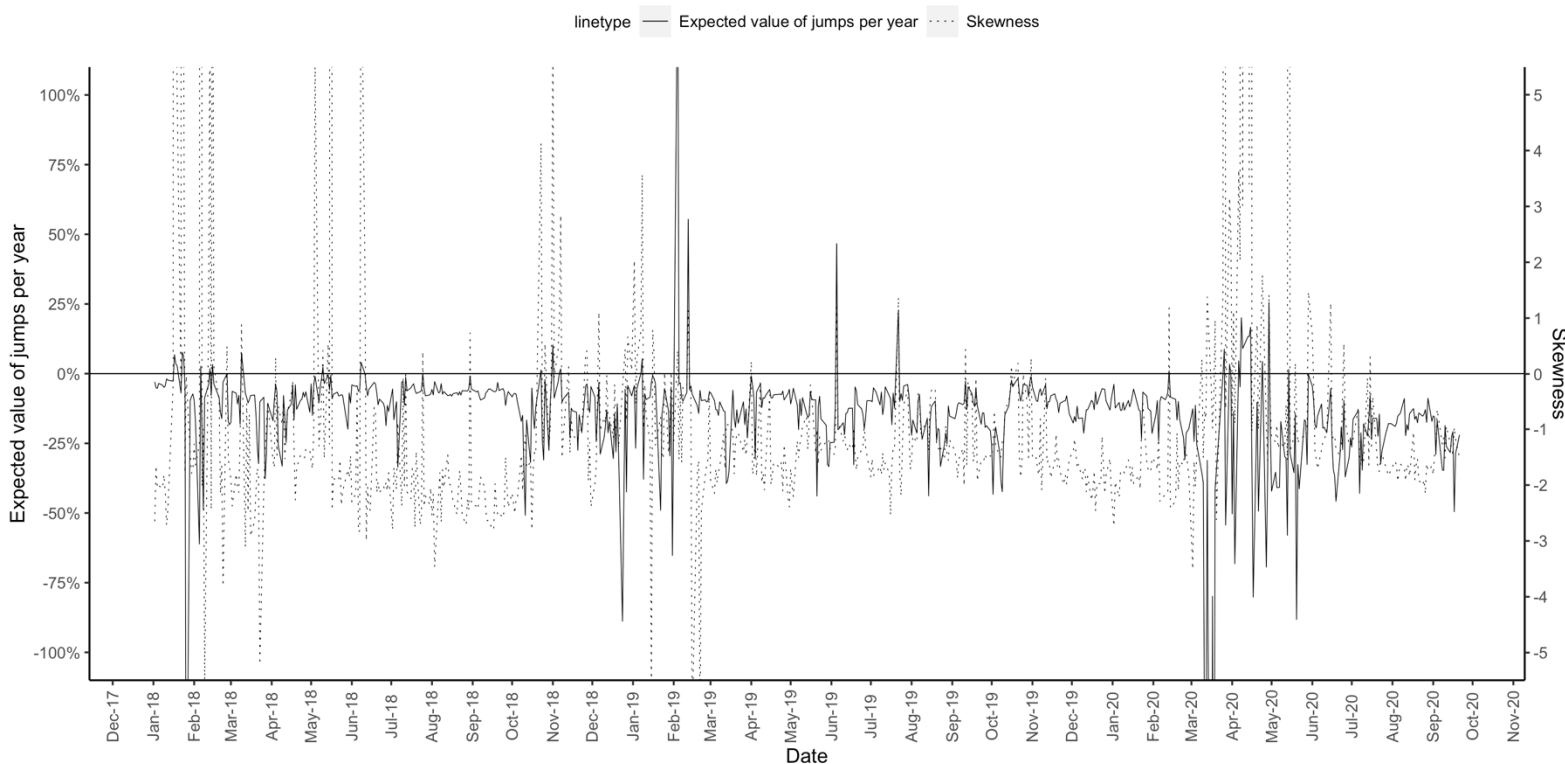


Figure 16. Risk-neutral expected value of jumps per year and the implicit skewness.

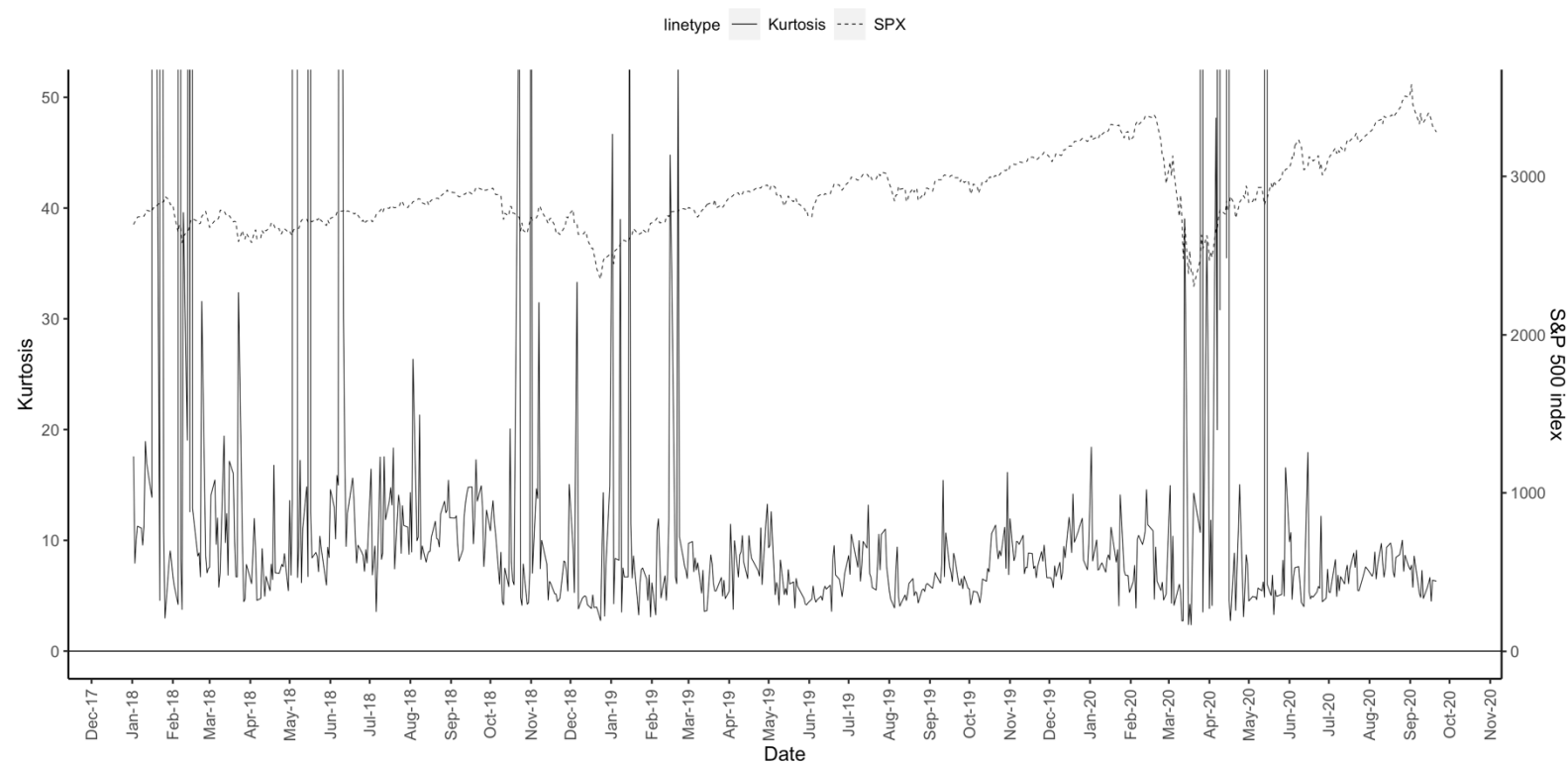


Figure 17. The implicit kurtosis of the risk-neutral return distribution of the S&P 500 index, and the index level.

The kurtosis is relatively low during March 19 – March, 20. It increases in March, when the market participants' expectations of negative jumps increase

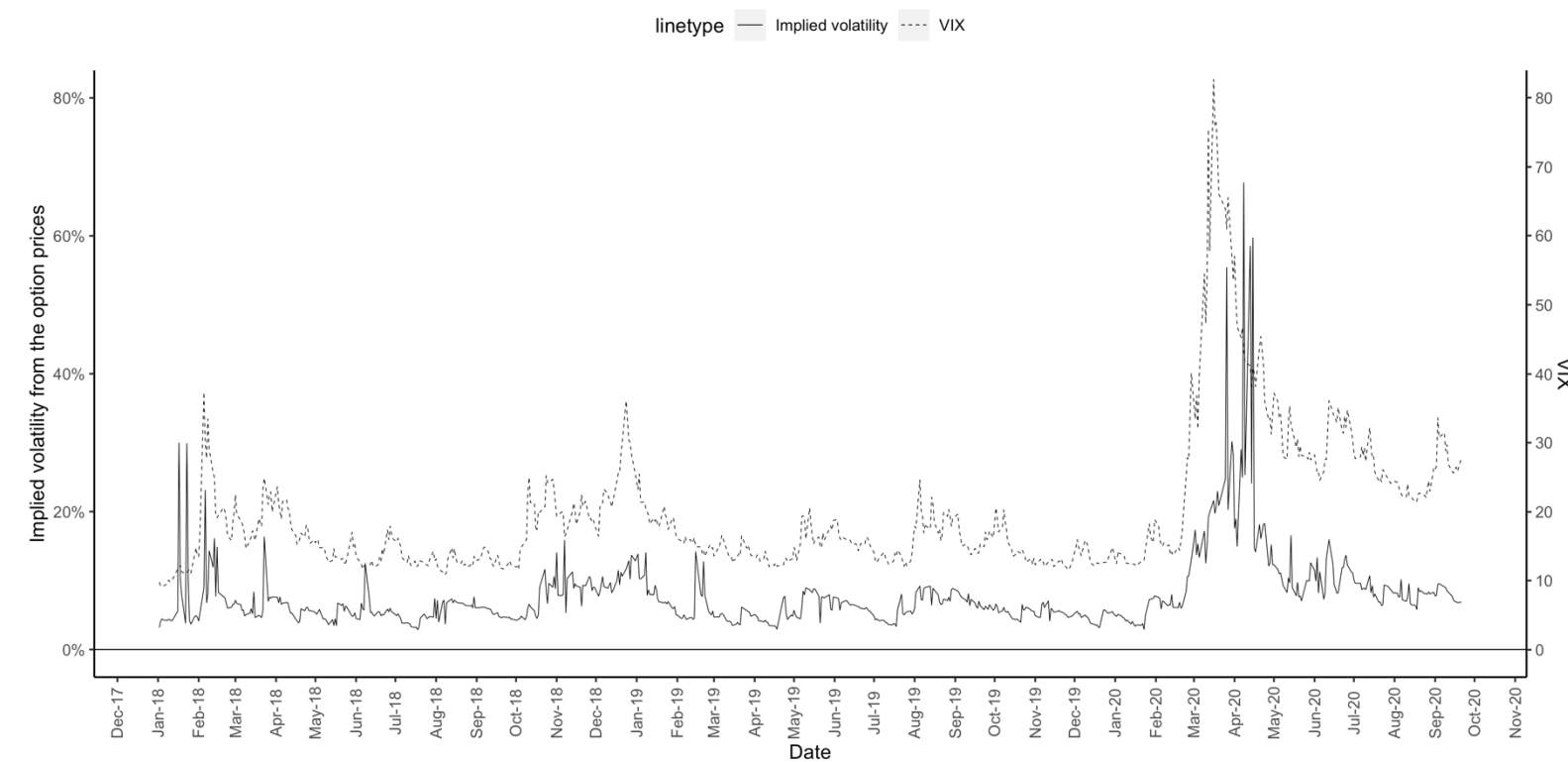


Figure 18. The estimated implied volatility and the VIX index. We observe that the estimated implied volatility and the VIX begin to increase in March 2020, and that they in general seem to move similarly over time

5. Limitations

There are possible limitations to our work that stems from the available data. First, there are some missing days in the dataset. As they are scattered throughout the observed time period, it will not limit our ability to observe the change in market expectations over time. It can on the other hand affect our ability to decide at what specific day certain effects appear, as the day may be missing which would lead us to believe that the effect appeared days later.

Second, if there are several options randomly missing, this might affect the level of efficiency in the findings from the option price data. As discussed in Section 2, there are call option prices missing. If the call price data is missing due to some systematic factor, it could lead to biased estimates. As an example, if it is only the most expensive call options per maturity that are missing, the estimated splines in the interpolation method would indicate a lower relationship between call price and strike price. This would lead to the calculated skewness premium being downward biased, thus invalid for representing the true level of the market expectations. With this said, we can still observe the *change* in market expectations over time if the systematic factor of the missing data holds for the entire period. If in contrast it changes with time, we cannot trust the estimated change of the skewness premium. If for example the most expensive calls are missing in 2018, while the cheapest are missing in 2019; all else being equal we would observe an increase in the skewness premium solely due to the difference in the missing data. If the option data is missing for random prices, we would not obtain such a bias, but it could still lower the precision of the estimates. As the data used in Part 2 is only a sample of the options used in Part 1, the same intuition applies in the case that the removed options have a systematic price difference relative to the options left out. There might also be an issue related to the moneyness of the chosen options. We choose the options with as evenly spread strikes as possible *after* the time to maturity is chosen. Hence, strike price variation for each day depends upon the options available for that maturity. If for example the maturity chosen for a specific day from the sample only includes the highest available strike prices of puts and lowest for calls, it could lead to all chosen options being ITM. Thus, they would not be a representative selection for all options that day. After inspecting the prices chosen on random days during the estimation, the strike prices for both puts and calls were in fact relatively evenly spread. Even though the options seem to be relatively evenly spread over strike prices for the inspected days, there might be days with less representative options.

Another uncertainty around the unbiasedness of the parameters estimated from the sample, is related to the sensitivities of the solutions from the objective function (10). As discussed in Section 4.2.2, different jump-parameters could yield the approximate same theoretical option prices. This implies that the solution when minimizing the objective function (10), might be very sensitive to the combination of the market prices and the theoretical prices. This is because there are very small amounts that distinguish the chosen solution for the estimated parameters each day in the estimation. On the other hand, from Figure 18 we can observe that the implied volatility found in the option prices from the sample moves similarly to the VIX over time. The VIX also begins to increase in March, indicating increasing crash fears among investors. This suggests that the inference drawn from our estimated jump-parameters, about when we can observe reactions in market expectations of jumps, is in fact reliable. We are interested in the *change* of the parameters over time, rather than the magnitude. Thus, we can argue that the inference about the changes in the market expectations of jumps drawn from the estimated jump-parameters is likely reliable.

For the first part of the study, calculating the skewness premium of the SPX options, we use cubic smoothing spline interpolation. One possible limitation to our work is if the interpolation method is not reliable during the observed time period. To ensure a continuous, monotone and convex relationship between $\frac{V_T}{F_T}$ and $\frac{X_T}{F_T}$, the degrees of freedom was set to 7 for the 2018 and 2019 data, while 5 for the 2020 data. The reason being that using 7 for the 2020 data makes the splines too sensitive for the observation variation, making the function non-monotonic and not convex. Decreasing the degrees of freedom makes the splines less sensitive to the variations. Using different restrictions on the degrees of freedom did not affect the inference from the changes in the calculated skewness premium. Having said this, making the splines less sensitive also makes them less representative for the observed prices.

By using data of several maturities to estimate the splines, we find the average of the skewness premiums for the distributions of different maturities each day. This increases the variance of the splines, especially after February 20, 2020. One of the reasons being that the market participants did not agree on how to price the options due to increased uncertainty, hence higher variance in splines for a single maturity. It is also due to the fact that the options with longer time to maturity were priced even higher relative to the ones with shorter time to maturity than before the crisis. Hence, using several maturities creates more noise in the

splines which may make it less representative for the actual prices. It does on the other hand also reflect a wider perspective of the skewness premium, with expectations on both shorter and longer term (within the range of 1- 4 months). By looking at the skewness premium of the ATM options, we can get an understanding of whether the interpolation method is reliable during the examined time period. In theory, the ATM skewness premium should be equal to zero. This is due to the expected payoffs of the corresponding call and put options both being 0. We observe that the calculated ATM skewness premium does in fact vary around 0, but the variance is quite large relative to the corresponding variance observed in Bates (1991). This may imply that the spline interpolation is not as reliable during the examined time period or that the mentioned distributional hypotheses does not hold. The observed standard errors of the estimated splines are quite low during most of the time before the market crash. This may be an indicator that the interpolation method is in fact reliable during this period. We observe from looking at the estimated splines, as the ones illustrated in Figure 5, that the splines seem to fit the data quite well during most of the time period before the crash.

6. Conclusions

The first case of Covid-19 in the U.S. was on January 20, 2020, a month before the first day of the large fall in the S&P 500 index. On March 23, the index was at its lowest after a fall of 34%. In light of this observation, the objective of our thesis was to examine whether there was any sign of increasing crash fears implicit in the SPX options prices, in the period before the stock market crashed. To answer this question, two methods are used based on Bates' (1991) study of the crash of 1987. The first method calculates the skewness premium of the 4% OTM and the ATM options. The second method estimates jump-parameters implicit in the options prices based on a diffusion that allows for asymmetric jumps.

In Part 1, we find that the put options trade at a premium relative to the corresponding call options during most of the time period examined. From Section 2 we know that the open interest is higher for put options than call options, suggesting that the price difference is explained by a higher demand for puts. We find that the skewness premium of 4% OTM options becomes less negative after February 20, 2020. It begins to decrease after March 16, the day when the S&P 500 index has its largest daily drop. This implies that the market participants first begin to buy protection in mid-March, meaning that the full impact of the crisis is not reflected in investor expectations of negative jumps until this point.

In Part 2, the estimated skewness fit the results from Part 1 in that it increases in the beginning of the crisis, but we do not observe a decreasing trend until April 2020. The implicit jump-parameters, implied volatility, skewness and kurtosis of the underlying risk-neutral return distribution, as well as the VIX index, imply that the reactions in market expectations do not fully begin until March 2020. At this point, the expected value of jumps becomes greatly negative, while the jump standard deviation and implied volatility increases.

Hence, we find that there is no evidence of increased crash fears in the market participants' expectations prior to the Covid-19 stock market crash. Our results indicate that the full impact of the crisis is not observed in market expectations of negative jumps until March 2020.

References

- A Decade Review of the S&P500 (SPX): Market Milestones. (2020, November 4). TradingView
<https://www.tradingview.com/chart/SPX/v1CLZgBM-A-Decade-Review-of-the-S-P500-SPX-Market-Milestones/>
- Bates, D.S. (1991). The Crash of '87: Was It Expected? The Evidence from Options Markets. *The Journal of Finance*, 43(3), 1009-1044.
http://pages.stern.nyu.edu/~dbackus/GE_asset_pricing/disasters/Bates%20crash%20JF%2091.PDF
- Black, F. & Scholes, M. (1973). The Pricing of Options and Corporate Liabilities. *Chicago Journals*, 81(3), 637-654.
https://www.cs.princeton.edu/courses/archive/fall09/cos323/papers/black_scholes73.pdf
- Compound Poisson process. (2020, June 25). *Wikipedia*.
https://en.wikipedia.org/wiki/Compound_Poisson_process
- Chicago Options. (2020). CBOE Volatility Index. Yahoo! Finance. [Data file].
<https://finance.yahoo.com/quote/%5EVIX/history?period1=1514764800&period2=1600819200&interval=1d&filter=history&frequency=1d&includeAdjustedClose=true>
- Gay, D.M. (1990). *Usage summary for selected optimization routines* (Computing Science Technical Report 153). <https://ms.mcmaster.ca/~bolker/misc/port.pdf>
- Gili, M. & Schumann, E. (2010, September). *A note on 'good starting' values' in numerical optimisation*. Comisef Working Paper Series No. 044.
https://www.uni-giessen.de/static_files/pcms/jlu/comisef/files/wps044.pdf
- Gormsen, N.J. & Kojen, R.S. (2020, August). *Coronavirus: Impact on Prices and Growth Expectations*. Becker Friedman Institute for Economics Working Paper No. 2020-22.
https://papers.ssrn.com/sol3/papers.cfm?abstract_id=3555917
- Hanke, M., Kosolapova, M., & Weissensteiner, A. (2020). COVID-19 and market expectations: Evidence from option-implied densities. *Economics Letters*, 195(109441), 1-4. <https://doi.org/10.1016/j.econlet.2020.109441>
- Jackwerth, J. (2020). What Do Index Options Teach Us About COVID-19? *The Review of Asset Pricing Studies*, 10(4), 618-634, <https://doi.org/10.1093/rapstu/raaa012>
- Kenton, W. (2019, February 17). *Kurtosis*. Investopedia.
<https://www.investopedia.com/terms/k/kurtosis.asp>

-
- Koehrsen, W. (2019, January 20). *The Poisson Distribution and Poisson Process Explained*. Towards data science. <https://towardsdatascience.com/the-poisson-distribution-and-poisson-process-explained-4e2cb17d459>
- Likos, P. (2020, October 9). *What is the CBOE Volatility Index (VIX)?* U.S. News & World Report. <https://money.usnews.com/investing/investing-101/articles/what-is-the-cboe-volatility-index-vix>
- Merton, R.C. (1973). An Inter-Temporal Capital Asset Pricing Model. *Econometrica*, 41(5), 867-887.
https://www.researchgate.net/profile/Robert_Merton/publication/4813202_An_Inter-Temporal_Capital_Asset_Pricing_Model/links/54d0b8120cf298d656683a7a/An-Inter-Temporal-Capital-Asset-Pricing-Model.pdf
- Ramelli, S. & Wagner, A. F. (2020). *Feverish Stock Price Reactions to COVID-19*. Swiss Finance Institute Research Paper No. 20-12.
https://papers.ssrn.com/sol3/papers.cfm?abstract_id=3550274
- Ross, S.M. (2010). *Introduction to Probability Models* (10th edition). Academic Press.
- Segal, T. (2020). *What Caused Black Monday: The Stock Market Crash of 1987?* Investopedia. <https://www.investopedia.com/ask/answers/042115/what-caused-black-monday-stock-market-crash-1987.asp>
- Solver. (n.d.). *Global Optimization Methods*. Frontline Solvers.
<https://www.solver.com/global-optimization>
- Summa, J. (2020, August 19). *Determining Market Direction With VIX*. Investopedia.
<https://www.investopedia.com/articles/optioninvestor/03/091003.asp>
- Tang, F. (2018). *Merton Jump-Diffusion Modeling of Stock Price Data* [Degree project, Linnaeus University]. Linnaeus University Press. <http://lnu.diva-portal.org/smash/get/diva2:1257256/FULLTEXT01.pdf>
- The Centre for Evidence-Based Medicine. (2020, 30, July). *The first case of COVID-19 in the USA*. <https://www.cebm.net/study/the-first-case-of-covid-19-in-the-usa/>
- The R Core Team. (2020). *R: A Language and Environment for Statistical Computing*. R Foundation for Statistical Computing.
<https://cran.r-project.org/doc/manuals/r-release/fullrefman.pdf>
- Wolfinger, M. (2020, September 22). *Learn About Volatility Skew*. The Balance.
<https://www.thebalance.com/volatility-skew-1-2536780>

World Health Organization. *Timeline: WHO's COVID-19 response.*

https://www.who.int/emergencies/diseases/novel-coronavirus-2019/interactive-timeline?gclid=Cj0KCQiAnb79BRDgARIsAOVbhRvpWfHDmBGkYHxau4loMcMC-T8ZJR5w3DQo5ZqwyjkUdQFCJGdj9UaAtvPEALw_wcB#

World Health Organization. (2020, 27, April). *Archived: WHO Timeline - COVID-19.*

<https://www.who.int/news/item/27-04-2020-who-timeline---covid-19>

Yan, G. & Hanson, F.B. (2006). *Option pricing for a stochastic-volatility jump-diffusion Model with log-uniform jump-amplitudes.* Proceedings of the American Control Conference 2006.

<http://homepages.math.uic.edu/~hanson/pub/GYan/acc06gyfbh10web.pdf>

2020 stock market crash. (2020, December 1). Wikipedia. Retrieved from:

https://en.wikipedia.org/wiki/2020_stock_market_crash